بنام خداوند جان وخرد کزو برتراندیشه برنگذرد

COULOMB EXCITATION AND BREAK UP

Marzieh Fatemian (Shadman–Valavi)

Linacre College, Oxford

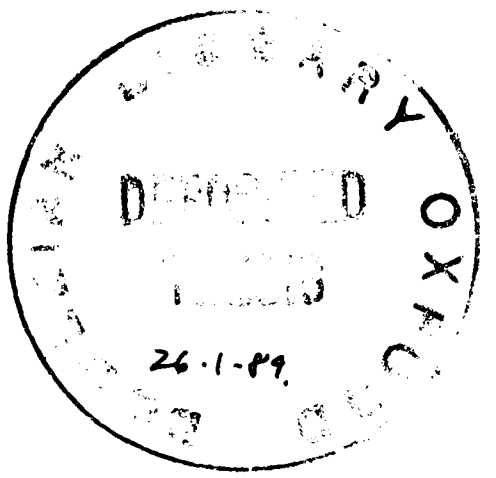

A thesis submitted for the degree of Doctor of Philosophy

at the University of Oxford

August 1988

تقدیم به پدر و مادرم

درخت تو گر بار دانش بگیرد بزیر آوری چرخ نیلوفری را

«ناصرخسرو»

COULOMB EXCITATION AND BREAK UP

Marzieh Fatemian (Shadman–Valavi)

Linacre College, Oxford

Submitted for the degree of Doctor of Philosophy

Trinity Term, 1988

Abstract

Break up processes involving a three body system in the Coulomb field are studied. A method is developed for the realistic treatment of such a system, and is applied to the break up of the nucleus, ^7Li. The Simple Cluster Model of ^7Li and the Coulomb excitation code COULVAR are used for the calculations. The continuum states of the $\alpha + t$ system are treated as a set of discrete states, by confining the relative motion of the clusters to a spherical box. The infinite set of states is then truncated by imposing an energy cutoff so that only the states below this energy are considered. The density of these states varies according to the box radius and the energy cutoff. The stability of the model is tested by varying these two parameters. The corresponding calculated probability of excitation of ^7Li has converged for a box radius of 20 fm and an energy cutoff of 20 MeV. The level energies and the wavefunctions of the continuum states are then easily obtained and are used to calculate the important matrix elements for the electromagnetic transitions between the bound states and the continuum states of ^7Li. The method is used to calculate the probability of excitation of ^7Li to its first excited state in the inelastic scattering experiments. It successfully reproduces a range of available data. An approximation is then developed to calculate the nuclear–Coulomb interference at low energies (well below the Coulomb barrier). The results of its application supports the need for renormalisation of the nuclear potentials suggested by inverse scattering calculations. The method closely reproduces The ^7Li data in this region with the refitted nuclear potentials. The application of the three body model to the break up of ^7Li on heavy targets at high energies produces very interesting results. It predicts reasonably good cross sections in the regions of pure Coulomb interaction. It also shows that at high energies the nuclear forces become very strong and affect the classical Rutherford orbit of the projectile. These effects are enhanced for heavier targets and the observed small scattering angle should not be taken as the angle of a classical orbit. Finally improvements towards the generalisation of the method are suggested so that it will be capable of coping with any three body system in a strong Coulomb field.

ACKNOWLEDGEMENTS

I would like to express my gratitude to my supervisor Dr B. Buck for his continual help and advice during my research work and also for the time he has spent reading this thesis during its preparation.

I was fortunate to have Dr D. M. Brink as my supervisor during Dr Buck's sabbatical leave. It was a pleasant experience to work with him and I am most grateful for his help and friendship.

It is my pleasure to thank Dr Richard Baldock for his invaluable assistance since I came to Oxford. He was a dependable source of help in times of disaster (and they were numerous!). He has kindly remained so even after moving to Edinburgh, and I greatly value his friendship.

I thank Prof. Sir Roger Elliott for awarding me a place in the Department of Theoretical Physics. I also thank all the members of the department who have made my time here an enjoyable one, especially the many good friends with whom I shared an office: Rachel, Fernando, Alberto, Gaynor, Hasnita, Peter and Luigi.

I wish to thank Ian McArthur and John MacAllister for their excellent maintenance of the Nuclear Physics Vax and their help in using it.

Finally I would like to express my thanks to all the members of my family for their love and support, especially to my parents for their love and encouragement; to my husband Ebby for sustaining me with his help, patience and love; to my sons Arash and Kaveh for their patience and undiminished love no matter how little they saw of me; to my younger sister Ensieh for her tremendous help during the past three years (which has provided me with plenty of peaceful time!); and to my uncle for producing the Persian writings with his computer.

CONTENTS

Chapter 1

INTRODUCTION

Coulomb excitation processes have been applied for many years (Huus and Zupančič, 1953; McClelland and Goodman, 1953) to the study of the electromagnetic properties of the low lying nuclear levels. In such a process the nucleus is excited by the electromagnetic field of a charged particle which does not penetrate into the region of nuclear force. Hence the nuclear properties enter only through the matrix elements of the electric and magnetic multiple moments of the nuclear states involved in the excitation. The nuclear properties that can be extracted from such study are the spin, parity and energy of the states as well as the electromagnetic matrix elements. In terms of these properties equations for cross sections, angular distribution etc. can be set up for any number of states.

With the advance of heavy–ion accelerators(1959) even more information could be obtained as multiple transition to higher states became possible . A measurable quantity corresponding to the probability of transition to any state may be defined as the reduced transition probability, $B(E\lambda)$, (Alder *et al*, 1956).

In multiple transitions it is possible to observe higher order corrections as well as $B(E\lambda)$.

One example of these higher order effects is the reorientation effect caused by an $E2$ transition between the magnetic substates of the final excited state. It was proposed by Breit *et al* (1956) that this effect can be used to determine the static quadrupole moment of the 2^+ state in $0^+ \rightarrow 2^+$ excitation of doubly even nuclei.

In principle it should be possible to extend this method to the odd nuclei where the first excited state or the ground state quadrupole moment can be measured. However this is not the only leading higher order effect and it was shown by Eichler (1964) that the second order E1 transitions via giant dipole resonance (GDR) results in an important contribution. Therefore any experimental attempt to measure the quadrupole moment by reorientation effect should take the virtual excitation into account.

In the case of odd nuclei when the ground state quadrupole moment is to be measured the first state which is strongly excited by the Coulomb force should have spin 1/2. Then its quadrupole moment is zero since there are no E2 transitions between the substates of a spin 1/2 state, and the reorientation effect corresponds to the quadrupole moment of the ground state. There are not many odd nuclei with this property and ^7Li offers a favourable candidate. Its first excited state $J^\pi = 1/2^-$ is at 0.478 MeV and the first state reachable via a virtual $E2$ transition is $\simeq$ 6 MeV higher. However in spite of these suitable conditions it contains a unique difficulty, namely the large coupling of the two low lying states to the $\alpha + t$ channel (Tombrello and Parker, 1963). As a result the $1/2^-$ state may be excited via the virtual break up of ^7Li.

In fact in a highly accurate experiment (within 1%) it should be possible to measure all 3 quantities; the reduced transition probability, the static quadrupole moment and the virtual break up effects. But the experiments carried out for this purpose (detailed below) did not provide a clear accurate measurement and furthermore, their measured values do not agree.

The quadrupole moment of ^7Li has also been measured by atomic spectroscopy (Green, 1971) and is therefore a less disputed value. The main discrepancy is between the measured $B(E2)$ ranging from 7.4 to 8.3 e^2fm^4 and the calculated values ranging from 6.26 to 7.42 e^2fm^4. But this apparent discrepancy is only due to the different treatments of the virtual break up states. The double E1 transition via these states interferes with the E2 transition in a destructive manner. Hence a small contribution from this excitation results in a large B(E2) value and vice versa. There have been two basic approaches to this problem: to treat the break up states as the states of a GDR or as the continuum states of the $\alpha + t$ system.

Bamberger *et al* (1972) analyse their data on the basis of $\alpha + t$ continuum states (Smilansky *et al*, 1972) and obtain the smaller $B(E2)$ value of 7.4. Häusser *et al* (1973) have analysed their data on the basis of the GDR treatment. The GDR effects are calculated using the hydrodynamic model (Winther, 1966; McDonald, 1964) but the result is a small contribution from virtual break up and hence the larger $B(E2)$ value of 8.3. The theoretical calculations which do not include virtual break up effects (Bouten and Bouten, 1981) predict the smallest $B(E2)$ value of 6.4. However none of these works presents a clear reliable method and they all have shortcomings, in one way or other.

The hydrodynamic model is only valid for heavy, doubly even nuclei which are well described by this model. But in light nuclei much larger polarizability is observed (Denisov *et al*, 1967) and the dominant particle–hole structure of the giant dipole resonance states cannot be ignored. Also in this model the probability of transition to the intermediate states is related to the (-2) moment of the photoabsorption cross section, but not all the states which contribute to the photoabsorption cross section take part in the double E1 transition to the $1/2^-$ state of ^7Li. For example the $5/2^-$ continuum state can not de–excite via $E1$ to the $1/2^-$ state. Furthermore the formula relating the probability of transition to the GDR states to the photoabsorption cross section is given for the case of $0^+ \rightarrow 2^+$ excitation. Häusser *et al* (1973) have tried to relate this to a formula for arbitrary spin but the result is a large $B(E2)$ value, that is, large compared to the values obtained by considering the continuum state of the $\alpha+t$ system.

There are strong factors leading to the conclusions favouring an $\alpha+t$ system rather than the GDR states. The experimental data (Tombrello and Parker , 1963) show a large overlap of the two low lying states with the $\alpha+t$ wavefunctions and also the break up threshold at 2.46 MeV is low.

The effect of E1 transitions to the continuum states of such a system can be calculated if the matrix elements for such transitions are known. However these transition matrix elements have not been available and the radiative capture cross section data have been used to extract these matrix elements. But the relative sign of the matrix elements, which is very important in the calculation, can not be determined from the data and it is derived under the assumption

that the low lying states are pure cluster wavefunctions (Smilansky *et al*, 1972). Another problem is that there are not sufficient data available and theoretical calculations are required to interpolate between the data.

Another way of calculating the effect of virtual break up is suggested by measuring the deviation of excitation probability from the first order calculated probability as a function of energy (Smilansky *et al*, 1972). But these observations require an assumed $B(E2)$ value to calculate the probability of the first order transition. Assuming a value of 7.0 e^2fm^4 , the results are very similar to the values obtained by using the E1 matrix elements mentioned above.

To clarify these discrepancies a Coulomb excitation experiment was carried out by Vermeer *et al* (1984). They measured the probability of excitation to the $1/2^-$ state of ^7Li by ^{208}Pb and^{138}Ba, in three independent experiments. Hence they could measure the three properties; the static quadrupole moment, the $B(E2)$ value and the virtual E1 break up effects independently. Their measured quadrupole moment is in a very good agreement with the atomic beam spectroscopy measurements. Their $B(E2)$ value of 7.42 e^2fm^4 is very close to the values obtained on the assumption of an $\alpha + t$ system. The virtual break up effect is measured in terms of a parameter k which is the ratio of actual GDR effects to those calculated from hydrodynamic model (Barker, 1982). They measure a value of $k = 2.7$ corresponding to the actual GDR effect being more than twice as large as it would be on the basis of the hydrodynamic model. These results are very useful in identifying the importance of the processes involved in such experiments and the best way to treat them.

At the same time a simple cluster model for ^7Li was developed (Buck, 1984; Buck *et al*, 1985) which predicted all the static properties of ^7Li successfully. It

is based on the assumption that the two clusters, α particle and triton, retain free space properties and interact via a deep local Gaussian potential. The potential parameters are fitted to reproduce level energies of the bound states of ^7Li and ^7Be. The model calculation yields a $B(E2)$ value of 7.42 e^2fm^4. This excellent agreement between the theory and the data (Vermeer *et al*, 1984) was the main motivation for the work performed for this thesis.

There was clearly a need for a proper treatment of the $\alpha + t$ system to reconcile all the experimental and calculated values of $B(E2)$. Such a need was also mentioned in a later work by Weller *et al* (1985). They calculated E1 effects by measuring the tensor analysing powers and obtained a value of 8.3 e^2fm^4 for $B(E2)$. They also mention an error in the Hartree-Fock calculations used to extract the value of the static quadrupole moment from atomic beam spectroscopy.

A reliable and proper calculation involving the continuum states of ^7Li would solve the problem of these uncertainties once and for all. Having such good agreement for $B(E2)$ between the data and theory provided an excellent test case for any such treatment. That is, on the basis of this agreement a calculation of the effect of continuum states of the $\alpha+t$ system, using the simple cluster model of ^7Li, should reproduce the measured excitation probabilities of Vermeer *et al.*

Such a model was also very much needed in the study of real break up of ^7Li. Earlier experiments on the break up of ^7Li by ^{208}Pb at 70 MeV (Shotter *et al*, 1981) suggested a strong involvement of Coulomb force in the direct break up component. However, a calculation based on the adiabatic approximation

for treating the continuum states yielded a better result if the nuclear forces alone were included (Thompson and Nagarajan, 1983). Further experiments on the break up of ^{7}Li by ^{120}Sn (Shotter *et al*, 1984) offered stronger evidence for the Coulomb break up at forward angles. This was confirmed by calculations based on the same principle as that used by Smilansky *et al* (1972) (mentioned above) using capture cross section data. A series of experiments was planned to study the Coulomb break up at forward angles and a realistic treatment of the continuum states would have been very useful in analysing these experiments.

The only method used so far to treat such a three body problem is the CDCC method [illegible]ura *et al* (1984). They discretise the continuum states using momentum bins and cutoff the angular and linear momenta. They are then able to perform a full coupled channel calculation involving these continuum states. Although they have successfully applied this method to many cluster–like nuclei their calculations do not, as yet, include the Coulomb interaction and therefore can not be used in the above cases, where the effect of the Coulomb force is required.

The aim of this thesis is to introduce a method to treat the continuum states of ^{7}Li as a system of two particles interacting with a third particle via the Coulomb field. This method is similar in principle to the CDCC model except that it deals specifically with the Coulomb force and does not include the nuclear interaction except as a perturbation.

The model used for ^{7}Li is the simple cluster model mentioned above. The continuum states are treated as an infinite set of discrete states obtained by confining the motion of the two clusters to a spherical box. This is a reasonable

assumption if the two clusters do not separate significantly during the interaction. This condition is satisfied if the ratio of the separation of the clusters to the distance of closest approach of ^7Li to the target is small, or if the collision time is small compared to the nuclear period, which is in fact the basic requirement also for a Coulomb excitation process to be dominant.

This infinite set of states is then truncated by an energy cutoff to enable the calculations to be performed with a finite number of states. The density of states within the box can also vary according to the radius of the box. Therefore these two values, the box radius and the energy cutoff, are the important parameters of this model. Their variation should result in the stability of the calculated value at some point, if the model is to be reliable. Once this has been tested then the energy of the continuum states and their wavefunctions can be easily calculated by numerical solution of the equation of motion.

The great advantage of this model is that any particular break up state can be obtained by imposing the appropriate boundary condition at the box radius. Now, if the total effect of transitions to all of these states is required then any convenient normalisation of these states is adequate. But if transition to a particular break up state is studied then that state should be normalised according to the given boundary condition, so that the superposition of a number of the continuum states corresponds to the specified break up state.

In chapter 2 the basic formulæ and parameters of a Coulomb excitation process are discussed and the formalism used in the semi–classical calculations of the excitation probabilities is presented. The Coulomb excitation code of Winther and De Boer (1966) which implements these formulæ is also briefly

discussed. The new version of this code , COULVAR (De Boer, 1978), is used throughout this thesis, modified, when necessary, to calculate the excitation cross sections and probabilities.

In chapter 3 the model for continuum states is introduced and explained in detail. Its validity and limitations are discussed together with its stability regarding the variation of the box radius and the energy cutoff. A rapid convergence of the probability of excitation to the first excited state is obtained at a box radius of 20 fm and an energy cutoff of 20 MeV. These results are very good and confirm the validity of the assumptions used for the model.

In chapter 4 the model is applied to the inelastic scattering of ^{7}Li and the results are compared with various experimental data mentioned above. The success of these results and the range of available data of Vermeer *et al* raised another interest. That is, the onset of nuclear–Coulomb interference was clearly marked and there were sufficient data beyond this point to test a method for calculating such interference.

Chapter 5 covers the detail of such calculations. The interference is well below the Coulomb barrier therefore it is assumed to affect only the excitation interaction and not the orbit. Then the tail of the nuclear potential may be included in the calculation as a perturbation to the Coulomb force while the Coulomb orbit is retained. The nuclear potential is then expanded in multipoles in the same way as the Coulomb force so that it can be easily added to the existing Coulomb excitation code. The results suggest a need for refitting the nuclear potential in the surface region. This is in agreement with the conclusions of the inverse scattering calculations of Mackintosh *et al* (1982–1986). The data is closely reproduced below the Coulomb barrier, using the refitted potentials.

Having established the reliability of the model for continuum states it is then applied to the real break up of ^7Li. Chapter 6 covers these calculations and the results are used to explain a range of available data by Shotter *et al* (1984-1987). These calculations show clearly the regions of pure Coulomb interaction and those with nuclear interference.

The summary of this work and suggestions for further development and application of the model are discussed in chapter7.

The work of chapters 3 and 4 has already been published (Fatemian *et al* , 1986). Chapter 5 is submitted for publication in the Phys. Lett. B and chapter 6 is being prepared for publication.

Chapter 2

COULOMB SCATTERING

2.1 Introduction

The term "Coulomb Excitation" is used for nuclear interactions where the Coulomb (electromagnetic) force alone, is responsible for any nuclear transitions. This is achieved when a target nucleus is bombarded by low energy charged particles. The low incident energy keeps the target and projectile sufficiently far apart that the short range nuclear forces can not act. But the electric interaction can excite the nucleus to a higher level and the projectile will then be inelastically scattered. In such a process the excitation of either the target or the projectile (or both) is possible.

Coulomb excitation cross sections are especially large for the nuclear collective states and so the Coulomb excitations have been used to test many collective models. Originally it was Bohr's collective model (1953) that stimulated the Coulomb excitation studies and they have since been an invaluable tool for investigating the nuclear excited states. The advantage of such investigation is

that only the well established theory of electromagnetic forces is involved and the complicated (and unknown) nuclear forces do not interfere. Furthermore relatively few states can be excited and therefore the calculations are easier.

In early experiments (1953–1959) only light projectiles such as protons or α–particle were used and the incident energy had to be very low to avoid strong interaction. This limited the number of states that could be studied and usually only single transitions were at all possible. But, with the development of Heavy–Ion Accelerators (1959), projectiles with much higher charge became available and a much greater range of states could be excited, often involving extensive multiple transitions. Such transitions complicate the situation but much more nuclear information can be obtained and in particular second order processes have been very useful in determining the quadrupole moments of excited states.

Another advantage of the Coulomb excitation process is that in general a full quantum mechanical treatment is not required. In most cases the motion of the particle is little disturbed by the loss of energy and it can be described by classical mechanics. Hence a "semi–classical" method is generally used for these calculations where the path of the particle is a classical hyperbolic orbit but the rest of the calculation is performed on the basis of quantum mechanics. As a result the Schrodinger equation of motion is solved for a classical orbit.

In this Chapter the basic theory of Coulomb excitation and a computer code related to this problem are presented. Section 2.2 describes the semi–classical methods and Section 2.3 deals with the mathematical formalism. In Section 2.4 some improvements to these calculations are discussed and Section 2.5 is a brief introduction to the code COULEX (Winther and De Boer , 1966).

2.2 Semi–Classical Method

In order to decide whether a classical description for a Coulomb excitation process is justified, one should compare the De Broglie wavelength, λ, with the dimension characteristic of the classical orbit, for example the distance of closest approach in a head–on collision, d. If $\lambda \ll d$ one can form a wave packet which moves along a hyperbolic orbit exactly like a classical particle. It is convenient to introduce the ratio between d and λ as a dimensionless parameter η which measures the strength of the Coulomb interaction, i.e.

$$\eta = \frac{Z_1 Z_2 e^2}{\hbar v} \tag{2.1}$$

where Z_1 and Z_2 are the charges of target and projectile and v is the incident velocity. In Coulomb excitation the velocity of the incident particle should be small enough to avoid nuclear penetration, therefore in the limit $\eta \gg 1$ a classical description of the projectile orbit is valid.

In addition if the energy of the state to be excited is small compared to the incident energy, the energy loss of the particle is negligible. Then the dominating force will be the Coulomb repulsion acting between the centres of charge of the target and the projectile. Hence the nuclear excitation is caused by the time dependent electromagnetic field acting on the nucleus while the projectile moves along a classical hyperbolic orbit.

Assuming that the incident particle starts from $r = -\infty$ at $t = -\infty$ the amplitude for the nuclear excitation when the projectile has reached $r = \infty$ at

$t = \infty$ can be calculated by solving the time dependent Schrodinger equation. The probability of excitation is the square of this amplitude and the inelastic scattering cross section is obtained by multiplying this probability by the Rutherford cross section.

However the differential equations for transition amplitude can not be solved analytically and numerical methods are required to obtain the solution. If the transition amplitudes are small, then first order perturbation theory can be used for their calculation.

2.3 Mathematical Formalism

The classical trajectory for a particle in the Coulomb field of a target nucleus is shown in Figure 2.1.

The Rutherford cross section is given by

$$\frac{d\sigma_R}{d\Omega} = \frac{1}{4}a^2 \sin^{-4}(\theta/2) \tag{2.2}$$

where a is the Coulomb parameter, defined as half the distance of closest approach in a head on collision, i.e.

$$a = \frac{Z_1 Z_2 e^2}{\mu v_p^2} \tag{2.3}$$

where μ is the reduced mass of the target and the projectile.

The differential cross section for nuclear excitation is given by

$$\frac{d\sigma}{d\Omega} = p\frac{d\sigma_R}{d\Omega} \tag{2.4}$$

where the probability p can be expressed in terms of the transition amplitude b_{if} connecting an initial state i to a final state f, i.e.

$$p = \frac{1}{2J_i + 1} \sum_{m_i m_f} |b_{if}|^2 \tag{2.5}$$

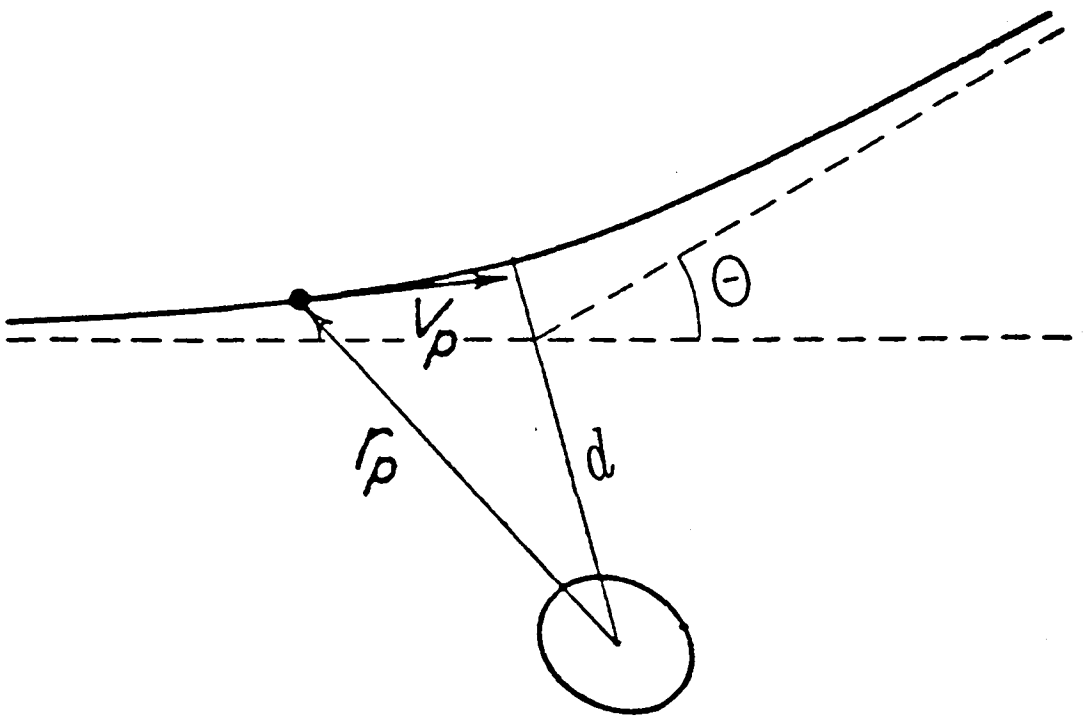

Figure 2.1

Rutherford orbit in the frame of reference in which centre of mass of target and projectile is at rest. $\mathbf{r_p}$ is the position vector of projectile relative to target and v_p is its velocity. θ is the scattering angle and d is the distance of closest approach.

where J_i is the spin of initial state and m_i and m_f are the magnetic quantum numbers of the initial and final states respectively.

The Schrodinger equation for the nuclear wavefunction is

$$i\hbar\frac{\partial\psi}{\partial t} = [\mathcal{H}_\circ + \mathcal{H}_E(t)]\psi \tag{2.6}$$

where $\mathcal{H}_\circ$ is the hamiltonian of the free nucleus and $\mathcal{H}_E(t)$ is the interaction energy. The function ψ can be expanded in terms of the eigenstates of $\mathcal{H}_\circ$ and a differential equation for the amplitudes is obtained (Alder and Winther 1960)

in the form

$$i\hbar \frac{db_m(t)}{dt} = \sum_n < m|\mathcal{H}_E(t)|n > e^{i\omega_{mn}t} b_n(t) \tag{2.7}$$

where $b_m(t)$ is the transition amplitude to the final state and

$$\omega_{mn} = \frac{E_m - E_n}{\hbar} \tag{2.8}$$

is the nuclear frequency.

Equation (2.7) should be solved with initial condition $b_n(t = -\infty) = \delta_{ni}$, to obtain the amplitude of a final state f arriving from the initial state i. Using first order perturbation theory (Dirac 1958) equation (2.7) is easily integrated and gives (Alder *et al*, 1956)

$$b_{if} = \frac{1}{i\hbar} \int_{-\infty}^{+\infty} < f|\mathcal{H}_E(t)|i > e^{i\omega_{fi}t} \tag{2.9}$$

The interaction energy $\mathcal{H}_E(t)$ is the electrostatic potential between the target and projectile, i.e.

$$\mathcal{H}_E(t) = \int \rho(\mathbf{r})\phi(\mathbf{r}, t)d\mathbf{r} \tag{2.10}$$

where $\rho(\mathbf{r})$ is the nuclear charge density and

$$\phi(\mathbf{r}, t) = \frac{Z_1 e}{|\mathbf{r} - \mathbf{r}_p(t)|} - \frac{Z_1 e}{\mathbf{r}_p(t)} \tag{2.11}$$

is the electrostatic potential. The second term in equation (2.11) is subtracted since it is responsible for scattering and does not contribute to the excitation, that is, it does not include a nuclear coordinate and hence it can not excite the nucleus.

$\rho(\mathbf{r})$ can be written in terms of point charge protons as follows

$$\mathcal{H}_E(t) = \sum_k e_k \phi(\mathbf{r}_k, t) \tag{2.12}$$

where e_k is the charge and r_k is the position vector of the kth nucleon with respect to the centre of mass of the target. Then using the multipole expansion of equation (2.11) one obtains

$$\mathcal{H}_E(t) = 4\pi Z_1 e^2 \sum_{\lambda\mu} \frac{1}{2\lambda+1} \frac{Y_{\lambda\mu}(\theta_p, \phi_p)}{r_p^{\lambda+1}} \mathcal{M}^*(E\lambda, \mu) \tag{2.13}$$

where

$$\mathcal{M}^*(E\lambda, \mu) = \sum_k r_k^\lambda Y_{\lambda\mu}(\theta_k, \phi_k) \tag{2.14}$$

Inserting (2.13) into (2.9) gives

$$b_{if} = \frac{4\pi Z_1 e^2}{i\hbar} \sum_{\lambda\mu} \frac{< J_i m_i | \mathcal{M}(E\lambda, \mu) | J_f m_f >}{2\lambda+1} S_{E\lambda,\mu} \tag{2.15}$$

where

$$S_{E\lambda,\mu} = \int_{-\infty}^{+\infty} e^{i\omega t} \frac{Y_{\lambda\mu}(\theta_p, \phi_p)}{r_p^{\lambda+1}(t)} dt \tag{2.16}$$

The matrix elements in (2.15) can be written in terms of the reduced transition probability $B(E\lambda)$ defined as (Alder *et al* 1956)

$$B(E\lambda; J_i \to J_f) = \frac{1}{2J_i+1} | < J_i \| \mathcal{M}(E\lambda) \| J_f > |^2 \tag{2.17}$$

and the cross section is then given by

$$\frac{d\sigma}{d\Omega} = \frac{4\pi^2 Z_1^2 e^2}{\hbar^2} \frac{a^2}{\sin^4(\theta/2)} \frac{B(E\lambda)}{(2\lambda+1)^3} \sum_\mu |S_{E\lambda,\mu}|^2 \tag{2.18}$$

The integrals $S_{E\lambda,\mu}$ are easily evaluated in a parametric representation using a particular coordinate system, i.e.

$$\begin{aligned} x_p &= 0 \\ y_p &= a(\varepsilon^2 - 1)^{1/2} \sinh(w) \\ z_p &= a(\cosh(w) + \varepsilon) \\ r_p &= a(\varepsilon \cosh(w) + 1) \\ t &= \frac{a}{v}(\varepsilon \sinh(w) + w) \end{aligned} \tag{2.19}$$

where ε is the eccentricity of the orbit, given by

$$\varepsilon = \frac{1}{\sin(\theta/2)} \tag{2.20}$$

In this system

$$S_{E\lambda,\mu} = Y_{\lambda\mu}(\frac{\pi}{2}, 0)\frac{I_{\lambda\mu}(\theta,\xi)}{av} \tag{2.21}$$

where

$$I_{\lambda\mu}(\theta,\xi) = \int_{-\infty}^{+\infty} \frac{[\cosh(w) + \varepsilon + i\sqrt{\varepsilon^2 - 1}\sinh(w)]^{\mu}}{(\varepsilon\cosh(w) + 1)^{\lambda+\mu}} e^{i\xi(\varepsilon\sinh(w)+w)} \tag{2.22}$$

ξ is the adiabaticity parameter defined as

$$\xi = \frac{a}{v}\frac{\Delta E}{\hbar} = \frac{Z_1 Z_2 e^2}{\hbar v}\frac{\Delta E}{2E} \tag{2.23}$$

This is the ratio between the collision time (a/v) and the nuclear period $(\Delta t = \hbar/\Delta E)$ and therefore it measures the extent to which the process is adiabatic.

$\xi = 0$ corresponds to a situation in which the nuclear period is long compared to the collision time and the process can be considered as sudden impact. Hence the sudden approximation applies.

$\xi \gg 1$ corresponds to an adiabatic process. For finite energy losses the process always becomes adiabatic for small angles and the Coulomb excitation cross section vanishes exponentially at forward angles.

For small values of ξ semi–classical formulæ can be used since the collision time is less than the nuclear period.

The calculations are now reduced to evaluating the orbital integrals $I_{\lambda\mu}$ and then the cross sections can be compared with data. The numerical values of $I_{\lambda\mu}$ are tabulated (Alder *et al*, 1956) for $\lambda = 1, 2, 3, 4$.

2.4 Improvements of Semi–classical Calculations

2.4.1 Magnetic Transitions

In the above calculations, only the electric transitions are treated. Magnetic transitions can also occur and a similar procedure (Alder *et al*, 1956) will give corresponding formulæ for the cross sections of such excitations. However since the velocity of the incident particle in a Coulomb excitation is small ($v/c \ll 1$) the magnetic transitions give negligible contribution.

2.4.2 Higher order processes

An important correction is due to the second order electric transitions. In the above calculations the perturbation theory to the lowest order was considered. In most cases this treatment is sufficient since the probability of a single transition is small. However the probability may become appreciable for high bombarding energies which may be used with high charge particles. Even when the probability is small the higher order effects may be important if the transition to the final state occurs via an intermediate state. These second order effects may also be treated on the basis of semi-classical theory.

The transition amplitude, b_{if}, for this case is

$$b_{if} = b_{if}^{(1)} + \sum_s b_{isf} \tag{2.24}$$

where $b_{if}^{(1)}$ is the first order amplitude, equation (2.9), and

$$b_{isf} = \frac{1}{(i\hbar)^2} \int_{-\infty}^{+\infty} e^{i\omega_{si}t} < f|\mathcal{H}_E(t)|s > dt \int_{-\infty}^{t} e^{i\omega_{fs}t'} < s|\mathcal{H}_E(t')|i > dt' \tag{2.25}$$

The summation in (2.24) is over all the intermediate states, s. Expression (2.25) can also be expanded to obtain formulæ similar to (2.18) for higher order cross sections (Alder *et al*, 1956). A more detailed discussion of such effects is given in Chapter 3, where the E1 transitions to continuum states of ^7Li are treated.

2.4.3 Symmetrised Orbits

In the above calculations the energy loss of the projectile is neglected and only the initial velocity is used instead of the velocity after excitation. It is expected that improved values for the excitation cross sections can be obtained if the initial and final velocities of the projectile are included in the calculations. Also it is possible to have Coulomb excitation to the states with high energies such that the energy loss of the projectile is not negligible but it is still small compared to the incident energy, so that the requirement for classical orbit is satisfied . Then this energy loss should be taken into account in order to obtain reasonable cross sections. This can be approximately done by using the symmetrised orbits.

The quantum mechanical calculations show that, in the classical limit where the probability of a single transition is small, the excitation cross section is symmetrical in v_i and v_f except for a factor of v_f/v_i (Alder *et al*, 1956). This symmetrization can be easily included in the calculations by using symmetrised parameters:

$$\begin{aligned} a &= \frac{Z_1 Z_2 e^2}{\mu v_i v_f} \\ \xi &= \frac{Z_1 Z_2 e^2}{\hbar}\left(\frac{1}{v_i} - \frac{1}{v_f}\right) \end{aligned} \tag{2.26}$$

Instead of those defined in (2.3) and (2.23).

The cross section formula, (2.4), should now be replaced by

$$\frac{d\sigma}{d\Omega} = \frac{v_f}{v_i} p \frac{d\sigma_R}{d\Omega} \tag{2.27}$$

and the corresponding a and ξ in expressions connected to p and $\frac{d\sigma_R}{d\Omega}$ are as defined in (2.26). Such symmetrization reproduces the quantum mechanical cross sections within a few percent when η is as small as 3 or even when ξ is as large as 2. The latter corresponds to a collision in which the incident particle loses more than half of its energy and the unsymmetrised cross section would be wrong by a factor of 100 or more (Alder *et al*, 1956).

When a calculated cross section is compared with data, the possible errors due to various approximations should be known so as to be able to extract accurate nuclear information. The corrections to the semi–classical approach have been studied by various authors and the final result is always close to that of a symmetrised orbit correction (Sukumar and Brink, 1983; Dos Aidos, 1983).

2.5 Coulomb–Nuclear Interference

The above calculations give satisfactory results only well below the Coulomb barrier. But at energies near the barrier the nuclear forces begin to have some effect on the interaction. At these energies one might still be able to calculate the excitation cross sections on the basis of the semi–classical approach. That is, to assume that the Coulomb orbit is not greatly affected by nuclear forces and to include the tail of the nuclear potential in the excitation interaction. This is of course only valid for energies below the Coulomb barrier but should improve the results for these cases. A more detailed application of such improvements is discussed in chapter 5.

2.6 A Code for Coulomb Excitation

COULEX (Winther and De Boer, 1966) is a computer code which solves the differential equations (2.7) numerically and calculates the excitation probabilities to the excited states, and the corresponding cross sections. The coordinate system and parametric representations, described in (2.19) , are used to simplify the calculations. The symmetrised parameters, (2.26), are employed in the code; therefore the calculated cross sections can be compared directly to data. The code requires an input parameter which determines the accuracy with which the final probabilities are calculated. This parameter is also used to adjust the step length of the integration routine. The total probability is checked every few steps and a warning is given when this total exceeds unity by 20 times the accuracy parameter. Hence it is possible to track sources of errors in the calculations. This original code only calculates E2–transitions for up to 10 nuclear states but an improved version, COULVAR (De Boer, 1978), calculates all the multipole transitions E1–E6 and M1–M6 for up to 30 nuclear states. The number of excited states can be easily increased by changing only three aray dimensional parameters, although the code was found to contain an error corresponding to these parametrisations as will be discussed in chapter 6. All the nuclear information, including the transition matrix elements, is provided as input data. COULVAR has been used and modified, when necessary, for all the Coulomb excitation calculations performed for this thesis. Perhaps it should be mentioned that it is important to make sure that the input matrix elements follow the same definition as the code, and to note that COULEX and COULVAR use different definitions for reduced matrix elements (that is they

have opposite signs). All the other formulæ and calculations are the same. The best background for the definitions and formalism used in COULVAR is given by Alder and Winther (1975).

Chapter 3

A MODEL FOR CONTINUUM STATES OF ^7Li

3.1 Introduction

The nucleus ^7Li has been extensively studied by Coulomb excitation. Its ground state $J^\pi = 3/2^-$ and its first excited state $J^\pi = 1/2^-$ at 0.478 MeV are connected by a strong E2 transition. In addition it has other interesting properties which can be measured by its inelastic scattering from heavy targets, leaving the target in its ground state. The choice of heavy target enables a Coulomb excitation process to be performed at higher energies. This involves higher order processes and transitions via the intermediate states. As mentioned in chapter 1 one of the interesting higher order processes is the reorientation effect, namely the transition between the magnetic substates of an excited state. The probability of Coulomb excitation to an excited state depends, in first order, on the $B(E\lambda)$ for that transition and in second order on the static quadrupole moments of the states,Q. The reorientation effect can be measured experimentally using heavy–ion projectiles, in order to extract the static quadrupole moment (De Boer and Eichler, 1968) . In ^7Li the first excited state. has

spin 1/2 therefore no quadrupole moment, so the two measurable quantities are $B(E2; 3/2^- \rightarrow 1/2^-)$ and $Q_{3/2^-}$. Therefore two independent sets of measurements of the probability of Coulomb excitation to the $1/2^-$ state should be sufficient to determine values of $B(E2)$ and $Q_{3/2^-}$; for example, excitations at two different bombarding energies or at two different scattering angles or for targets of different charge.

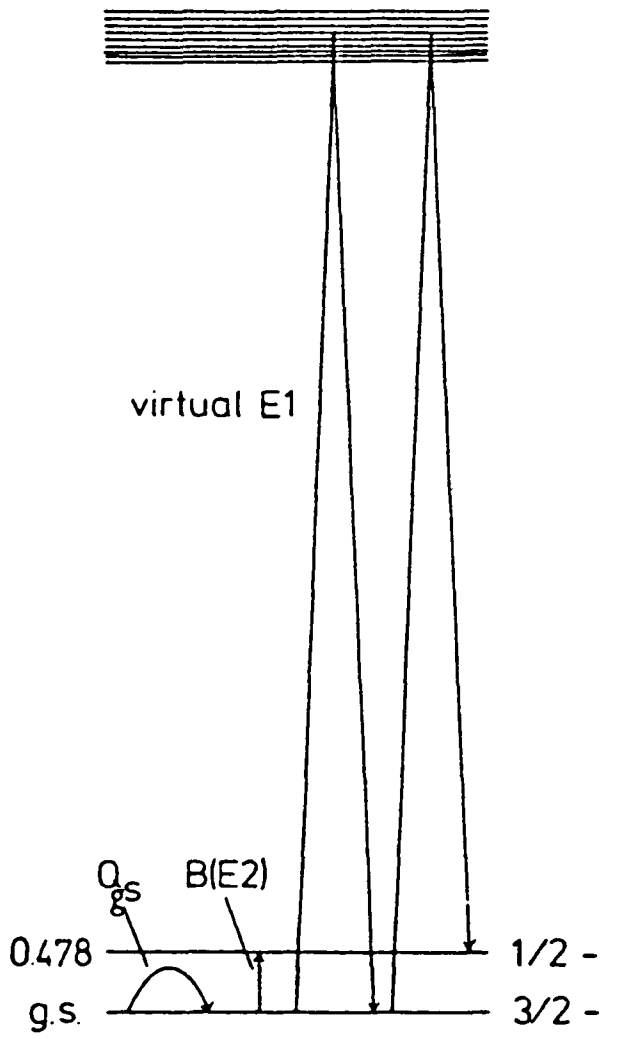

Figure 3.1
Schematic representation of energy levels of ^7Li. The measurable quantities associated with various transitions are shown.

However the particular structure of ^7Li causes a great difficulty in these measurements and although the measured and calculated values of $Q_{3/2^-}$ agree within experimental errors there is a discrepancy between the various measured values of $B(E2)$ as well as the calculated values. This is due to the importance

of another second order effect, namely virtual excitation to the continuum states (Figure 3.1).

In fact the virtual break up affects both the measured values, $B(E2)$ and $Q_{3/2^-}$. The inclusion of this effect is very important in the analysis of the experimental data and it must be included in the calculations aiming to describe the scattering data.

Due to the low $\alpha+t$ threshold (2.46 MeV) the transition to continuum states is strong in all Coulomb excitation processes of ^7Li. An E1 transition to the continuum states followed by an E1 decay to $1/2^-$ state contributes an effective E2 strength to this state. Therefore it should be deducted from the measured E2 strength to obtain the correct strength corresponding to the $B(E2)$. Also, since the matrix elements for E1 transitions are large, a sizeable effect , comparable to the reorientation effect is expected. Therefore any experiment aiming to measure $Q_{3/2^-}$ by the reorientation effect should consider the virtual break up effects carefully.

However the main discrepancy is between various measured values of $B(E2)$. This apparent discrepancy is in fact due to the different methods of including the virtual break up effects in the analysis of Coulomb excitation data.

Treating the continuum states reached by E1 excitation as components of a giant dipole resonance (GDR) has been successful for heavy doubly even nuclei (DeBoer and Eichler, 1968) . For the special case of $0^+ \rightarrow 2^+$ excitation a formula relating the the sum over the intermediate states (second term in equation 2.21) to the (-2) moment of photonuclear absorption, σ_{-2}, is given.

This is an experimentally known quantity defined by

$$\sigma_{-2} = \int \frac{\sigma}{E^2} dE$$

and is empirically given by Levinger (1957). The excitation via GDR states can also be treated on the basis of the hydrodynamic model (Winther, 1966). It is assumed that the initial and the final states can be described in terms of the collective excitation of the nuclear surfaces and that the giant dipole resonance is built on these states. However the hydrodynamic model is not valid for the light nuclei as the particle–hole structure is dominant in the giant dipole resonance states and an estimate of E1 polarization effects should be made by a more complete treatment of these states. The inadequacy of the model for light nuclei is also confirmed by the measured photoabsorption cross section. Ahrens *et al* (1975) have measure a value of $\sigma \simeq 0.196 mb/MeV$ whereas the empirical value mentioned above gives a value of $\sigma \simeq 0.089 mb/MeV$; less than half the measured value. Häusser *et al*(1973) have applied this method to the analysis of their data and have obtained a $B(E2)$ value of 8.3 $e^2 fm^4$.

Another approach is to treat the continuum states as the states of the $\alpha + t$ system since this is the only important breakup channel in Coulomb excitation. Then the required matrix elements corresponding to transition to these states should be calculated. To avoid solving a three body problem these matrix elements have been calculated using the fusion data (Smilansky *et al*, 1972). But since there are not sufficient data available for these calculations the data should be interpolated as required. This may affect the accuracy of the calculated matrix elements. This method results in a lower $B(E2)$ value, 7.4 $e^2 fm^4$ (Smilansky *et al*, 1972; Bamberger *et al*, 1972).

In an accurate enough experiment (within 1%) all three quantities; $B(E2)$, $Q_{3/2-}$ and E1 polarization are measurable. Vermeer *et al* (1984) have measured these quantities in three independent experiments hence determining these values in a model independent way. In fact the extraction of the E1 effects still depends on an assumption about the form of the polarization but they measure a ratio k, defined by Barker (1982) as the ratio of the actual GDR effects to that obtained from the hydrodynamic model. They measured a $B(E2)$ value of 7.42 e^2fm^4, a $Q_{3/2-}$ value of -4 ± 1 efm^2 and a value for $k = 2.7$. this confirms the idea that the hydrodynamic model underestimates the virtual break up effects. The experimental evidence for the strong coupling between the low lying states of ^7Li and the $\alpha + t$ continuum states (Tombrello and Parker 1963) and also the low $\alpha + t$ threshold at 2.46 MeV were already strongly in favour of the second method mentioned above and these experimental results also confirmed it. However calculation of the matrix elements for the transitions to the continuum states of the $\alpha + t$ system involves three body wavefunctions and is correspondingly more difficult.

This kind of problem has been studied by Yahiro *et al* (1982), where the $p+n$ continuum states of the deuteron are investigated. They employ a method to discretise the continuum states which are then used to perform coupled channel calculations. This so called Coupled–Discretised–Continuum–Channel (CDCC) method has also been applied to the breakup states of ^6Li, ^7Li and ^{12}C (Kamimura *et al*, 1984). However these calculations only involve the nuclear interaction and therefore are not useful where the Coulomb force is dominant, i.e. in a virtual Coulomb excitation process or in a Coulomb break up. The method

presented here solves this problem and deals with a three body interaction involving a strong Coulomb force. It is based on the Simple Cluster Model (SCM) of ^7Li (Buck *et al*, 1985) which is briefly discussed in Section 3.2. In Section 3.3 the method itself is detailed and its mathematical formalism is considered in Section 3.4. Section 3.5 is a discussion of the validity and the limitations of the method.

3.2 Simple Cluster Model

The application of this model to A=7 nuclei shows excellent agreement for all the static properties and some resonance widths, and also correctly predicts the important astrophysical S–factor for production of ^7Be. It is assumed that the two clusters in ^7Li, i.e. the α particle and the triton, have their respective free space properties and interact via a deep local potential of Gaussian shape. The minimum number of nodes of the relative wavefunction is determined by the Pauli principle. That is, good cluster states can only exist if the Fermi spheres of the two clusters do not overlap. Therefore the total quantum number, N, is given by the"Wildermuth" condition (Wildermuth, 1958 and Rubio, 1984)

$$N = 2n + L = \sum_{i=1}^{n_c} (2n_i + l_i) \tag{3.1}$$

where n is the number of nodes in the relative wavefunction, L is the relative orbital angular momentum, n_c is the number of nucleons in the lowest shell model configuration and n_i and l_i are the single particle quantum numbers. For ^7Li, the lowest configuration allowed is $(0s)^4(0p)^3$, which gives $2n + L = 3$ or $L = 1$ and $L = 3$. The spin–orbit coupling for the triton ($J^\pi = 1/2^+$)

results in $J^\pi = 3/2^-, 1/2^-$ for the ground state and the first excited state and $J^\pi = 7/2^-, 5/2^-$ for higher resonance states. The Gaussian potential is parity dependent and the parameters for odd parity states are chosen to reproduce the ground state doublet of ^7Li and ^7Be at the correct positions and $< r^2 >$, the mean square separation between the centres of mass of the clusters. The assumed potential has the form

$$V(R) = -(V + 4\alpha V_{so}\mathbf{L}.\sigma)exp(-\alpha R^2) + V_C(R)$$
$$V_C(R) = \begin{cases} Z_1 Z_2 e^2/R & R > R_C \\ (Z_1 Z_2 e^2/2R_C)(3 - (\frac{R}{R_C})^2) & R < R_C \end{cases} \tag{3.2}$$

The four parameters i.e. V, α, V_{so} and R_C (Coulomb radius) are uniquely determined by the above requirements (Buck *et al*, 1985). The position of the $L = 3$ doublet may be fitted by increasing V_{so} and then the phase shifts for $\alpha + t$ elastic scattering are accurately produced. The even parity potential is determined by considering the S–wave phase shifts. Assuming the same shape for the potential its central depth,V, is varied to obtain the best fit phase shifts. Hence the even parity potentials have the same parameters as the odd parity potentials except a smaller depth. In general both the depth and the shape could be varied to obtain the same best fit results.

3.3 Continuum States

The continuum states of the $\alpha + t$ system are treated as the set of states obtained from the relative motion of the two clusters in a spherical box. It is possible to confine the clusters in a spherical box if the relative kinetic energy in the breakup channel is small and hence the two clusters do not separate significantly during the interaction. The collision time for a head–on collision is

given by a/v which for 20 MeV ^7Li on ^{208}Pb is of the order of 10^{-22} sec. The $\alpha - t$ relative energy is $\simeq 3$ MeV and the separation of the clusters corresponding to the distance travelled by the relative energy during the collision time is $\simeq 1.8$ fm. The mean square radius of ^7Li is 13.5 ± 0.3 fm^2, hence the separation is not significant and the idea of confining the clusters in a spherical box is reasonable.

Enclosing the system results in the description of the relative wavefunction by means of a complete discrete set. So far no approximation has been used but in order to make the calculation possible the infinite set of continuum states should be truncated to obtain a finite number of state. Therefore a restriction is imposed by introducing an energy cut off, E_c, which is the maximum energy of the discrete states.

The advantage of this model is that by varying the boundary conditions any particular state can be produced. The discrete wavefunctions are normalised individually, within the box volume. If the total effect of transitions to continuum states is considered such normalisation is adequate, that is, imposing a different boundary condition will yield a different set of states but the total strength of the transitions to all these states will be the same. However if a particular breakup state is required then the normalisation of the wavefunctions needs to be more carefully considered and it will be discussed later.

Although the energy cut off is the only approximation involved, changing the box radius, r_b, also affects the density of discrete states. Hence these two parameters, r_b, and E_c must be carefully studied so that the accuracy of the method can be assessed. In particular the sensitivity of the required excitation probabilities to these parameters must be determined. This has been explicitly tested and will be discussed further in Section 3.5.

At this stage it is interesting to draw attention to the similarity of this method and the CDCC method mentioned above. In CDCC the infinite set of states is truncated by introducing a momentum cut off, i.e. states with $k \leq k_{max}$ and $l \leq l_{max}$ are considered where k and l are the linear and orbital angular momenta respectively. This truncated set is then discretised into momentum bins of width Δk. Again varying k_{max}, l_{max} and Δk will increase the number of states and they found sufficient and smooth convergence of S matrix elements at $l_{max} = 2$, $k_{max} = 1$ and $\Delta k = 1/8$ fm^{-1} for the deuteron. One could compare the momentum cut off, k_{max}, which truncates the infinite set, to the energy cut off in the method described here which has the same effect. The momentum bin Δk seems to be analogous to the effect of box radius r_b. If one relates ΔE, separation between energy levels in this method, to Δk of CDCC then for a given E_c the variation in r_b results in variation in ΔE which is equivalent to the effect of varying Δk. However the CDCC method has an extra restriction, namely the angular momentum cut off, l_{max}, which restricts the virtual transitions and may in fact underestimate the contribution from the continuum states.

3.4 Mathematical Formalism

The interaction involved in Coulomb excitation has been described in Chapter 2 and the required matrix elements can easily be calculated in terms of Clebsch–Gordan coefficients and radial integrals as follows:

The cluster wavefunction can be written as

$$|JM>=\sum_{m\sigma} < L\ 1/2\ m\sigma|JM > |Lm > |1/2\ \sigma > \qquad (3.3)$$

The reduced matrix elements are defined (Brink and Satchler, 1968) as

$$< J_f M_f | \mathcal{M}_{\lambda\mu} | J_i M_i >= (-1)^{J_f - M_f} \hat{J}_f \begin{pmatrix} J_f & \lambda & J_i \\ -M_f & \mu & M_i \end{pmatrix} < J_f \| M_\lambda \| J_i > \quad (3.4)$$

where $\hat{J}_f = \sqrt{(2J_f + 1)}$.

The cluster operator is defined (Rubio 1984) as

$$\mathcal{M}_{\lambda\mu} = \beta_\lambda r^\lambda Y_{\lambda\mu}(\hat{\mathbf{r}}) \quad (3.5)$$

with

$$\beta_\lambda = Z_1 (\frac{-A_2}{A})^\lambda + Z_2 (\frac{A_1}{A})^\lambda \quad (3.6)$$

Z_i and A_i are the charge and the mass of the ith cluster.

There is no spin operator therefore $\mathcal{M}_{\lambda\mu}$ acts on the radial part only. Hence (Brink and Satchler, 1968)

$$< L_f \ 1/2 \ J_f \| \mathcal{M}_\lambda \| L_i \ 1/2 \ J_i >= J_i L_f (-1)^{\lambda + L_i + J_f + 2L_f + 2J_i + 1/2} \times W(J_f J_i L_f L_i; \lambda \ 1/2) < L_f \| \mathcal{M}_\lambda \| L_i > \quad (3.7)$$

and

$$< L_f \| \mathcal{M}_\lambda \| L_i >=< L_f \| Y_\lambda \| L_i >< r^\lambda >_{fi} \beta_\lambda \quad (3.8)$$

where

$$< r^\lambda >_{fi} = \int r^\lambda u_f u_i dr \quad (3.9)$$

u_f and u_i being the radial wavefunctions of the final and initial states respectively. Using the coupling of spherical harmonics (Brink and Satchler, 1968)

$$< L_f \| \mathcal{M}_\lambda \| L_i >= \frac{\hat{L}_i \hat{\lambda} \beta_\lambda}{\sqrt{4\pi} \hat{L}_f} < r^\lambda >_{fi} < \lambda L_i 00 | L_f 0 > \quad (3.10)$$

Inserting (3.10) into (3.4) and comparing with the definition of reduced matrix elements in COULVAR, one obtains the following expression as required by COULVAR

$$< J_f \| \mathcal{M}_\lambda \| J_i >= \frac{\hat{\lambda}\beta_\lambda}{\sqrt{4\pi}} \hat{J}_f \hat{J}_i \hat{L}_i (-1)^{\frac{1}{2}-\lambda+L_i-J_f} < r^\lambda >_{fi} W(J_f J_i L_f L_i; \lambda \frac{1}{2}) \tag{3.11}$$

Now the only ingredients needed are the wavefunctions, u_f and u_i.

The bound state wavefunction is calculated by numerical integration of the radial equation of motion

$$u''(r) = \frac{2m}{\hbar^2}(V - E)u(r) \tag{3.12}$$

where

$$V = V(R) + \frac{\hbar^2}{2m}\frac{l(l+1)}{r^2} \tag{3.13}$$

and $V(R)$ is the sum of the Coulomb potential and the Gaussian potential of the SCM (equation 3.2).

The resonance state wavefunction can also be treated as a bound state. The sharp resonance states are obtained when the energy is just greater than zero i.e. $0 < \quad E << V$ (Blatt and Weisskopf, 1952). Therefore if the potential is rounded off at the top of the barrier then states of positive energy are produced which are bound but their wavefunctions simulate those of resonance. Therefore a rounded off potential is used in equation (3.12) to calculate the energy levels and wavefunctions of resonance states.

The continuum state energies are calculated by scanning an energy range $0 - E_c$ in very small intervals to find the energies at which the wavefunctions go

to zero at the box radius or in general for where the given boundary condition is satisfied. Then the wavefunction is calculated as for bound state with known energy.

In fact a resonance state can also be calculated by the method for the continuum states as it is in the continuum region. But a specific normalisation is required to obtain this state. A resonance is the sharp narrow peak observed in the excitation function (Jackson, 1970). At sufficiently high energies the widths of these peaks become much greater than the average spacing and the resonances overlap resulting in a much smoother excitation function. If these fine structures are not resolved a broad maxima is observed in the excitation function. In a single-particle potential model of the nucleus a resonance will occur when the incident energy corresponds to a quasi-bound state of the particle moving with positive energy. This is the procedure used above for calculation of the resonance states. The method which calculates the continuum states in fact resolves these resonances over a wide energy range. Therefore in order to obtain a particular break up state these levels should be normalised such that their superposition consists of a peak corresponding to the required state and a smooth background.

3.5 Discussion of E1 transition matrix elements

The matrix elements for transitions between $L = 1$ states $(3/2^-, 1/2^-)$ and $L = 0$ states $(1/2^+)$are calculated as explained above and the effects on the probability of excitation $(3/2^- \rightarrow 1/2^-)$ of ^7Li are obtained for a range of box radii, r_b and cut off energies, E_c. The excitation of ^7Li scattered from ^{208}Pb at 171° with bombarding energy of 20 MeV is an example of a Coulomb

excitation process. The results for these calculations shown in Table 3.1, are strong evidence for the validity and usefulness of the proposed model for the continuum states.

	10(fm)	15(fm)	20(fm)	30(fm)	40(fm)	60(fm)
10(MeV)	6.049	6.040	6.033	6.034	6.035	6.034
20(MeV)	6.042	6.033	6.030	6.031	6.030	6.029
40(MeV)	6.042	6.034	6.030	6.029	6.029	

Table 3.1

Table of $10^3 \times p(3/2^- \rightarrow 1/2^-)$ for a typical case; $\mathrm{E}(^7Li) = 19.483$ MeV & $\theta = 171°$, $10^3 \times p_{exp} = 5.27 \pm 0.05$. Row labels are the energy cut off, E_c, and column labels are the box radius, r_b.

Table 3.1 shows that the probabilities rapidly converge and the inclusion of the extra states due to larger r_b (>20 fm) and greater E_c (>20 MeV) has almost no effect on the excitation probability. These values for box radius and energy cut off are very reasonable i.e. they are large enough for the purpose of these investigations and yet small enough to enable the calculations to be performed within a reasonable computing time. Hence these values of $r_b = 20\ fm$ and $E_c = 20\ MeV$ are used for all the subsequent breakup calculations in this thesis.

The convergence is also evident and would be expected from the behaviour of wavefunctions of the discretised continuum states shown in Figure 3.2. As the box radius or E_c are increased the density of states is increased but the wavefunctions become more oscillatory outside the region of the bulk of the bound state wavefunction ($\simeq 7fm$). Hence the larger number of states inside

this region is compensated by this smaller amplitude and the total strength remains the same. There are two important points that should be mentioned here:

1) The calculational errors in the probabilities due to inclusion of breakup states, is also a check on the method. As mentioned in Chapter 2, a symmetrised orbit will give good cross section values, almost equivalent to an exact treatment of second order effects, even when the bombarding energy is comparable to the energy of the excited states. In the case of 20 MeV or smaller bombarding energy and E_c value of 20 MeV a few of the highest continuum states cannot be included in the symmetrised orbit calculations, i.e. a symmetrised Coulomb parameter (equation 2.26) is not possible. Hence COULVAR has been modified to use the unsymmetrised parameters for states with higher energy than the bombarding energy. The result is a small error (0.0002) in the total probability. So the calculated probabilities are still reliable.

2) The relative sign of E1 transition matrix elements is very important in these calculations, especially since it has to match the definition used in COULVAR. There is no independent way of checking these signs, since they can not be measured. But great care was taken in using various definitions of reduced matrix elements and angular momentum coefficients and a good deal of time was spent in making sure the calculated matrix elements have the correct sign rather than just relying on a sign which would result in the required destructive effect on $p(3/2^- \rightarrow 1/2^-)$.

As an extra check on the code it was run with the the best fit extracted from various experiments to see if the corresponding measured probabilities were

produced. COULVAR has the option of using a polarization term corresponding to the virtual break up effects. The polarization term is related to that used by Häusser *et al* and can also be related to the k measured by Vermeer *et al.* Hence the code can be used to calculate the excitation probabilities for a given $B(E2)$, $Q_{3/2^-}$ and E1 polarization effect. The results of both sets of data (Häusser *et al*, 1973 and Vermeer *et al*, 1984) were satisfactorily reproduced.

Having established the validity of the model, through the convergence of $p(3/2^- \rightarrow 1/2^-)$, one can suggest this technique for a proper treatment of breakup states. It is of course useful for all similar situations, not just the ^7Li system, which in this work is analysed to demonstrate the method. Various E1 transitions which might effect inelastic scattering and also other multiple transitions are considered in detail and discussed in the following chapter.

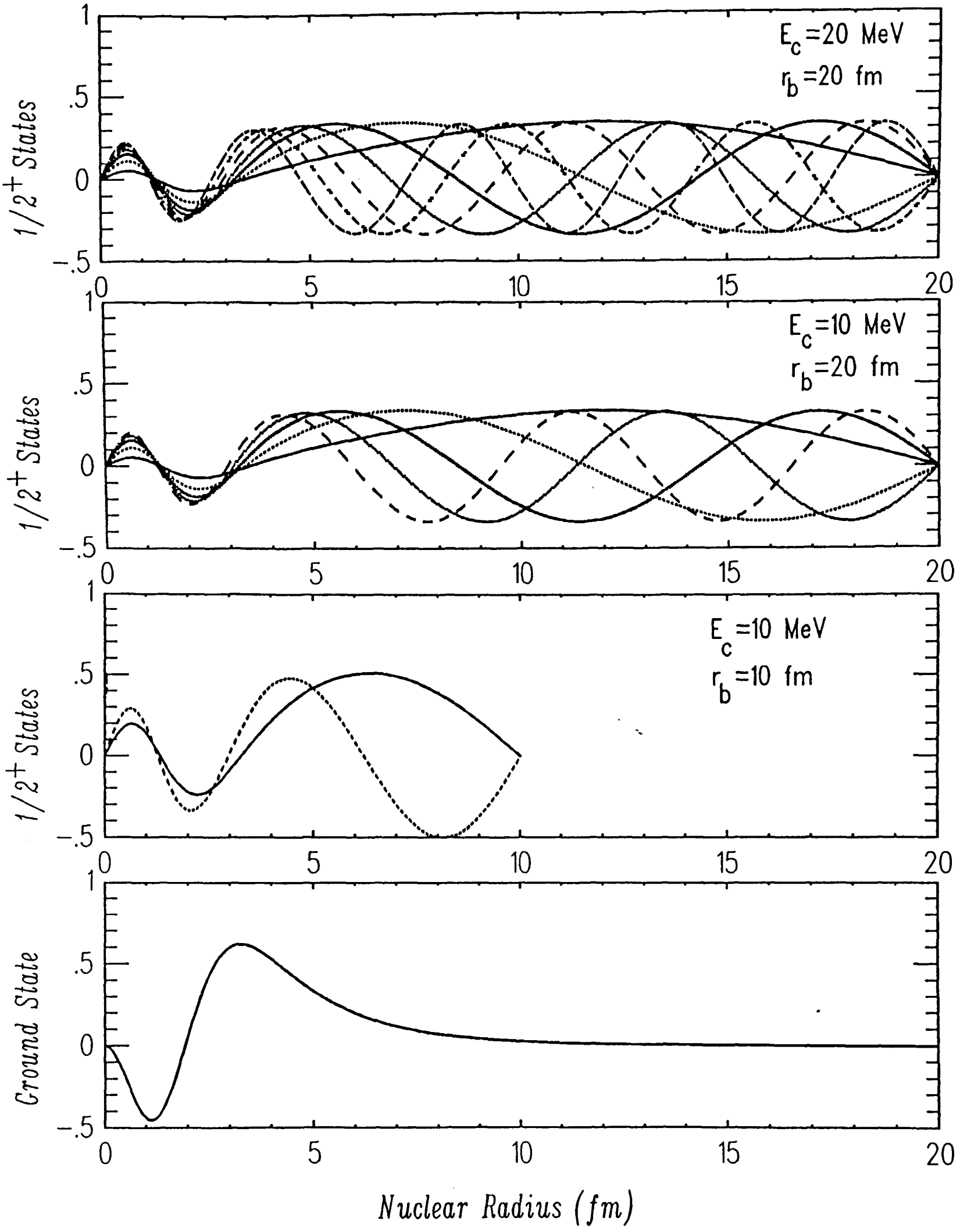

Figure 3.2

Wavefunctions of continuum states, for various box radii and cut off energies, compared to ground state wavefunction.

Chapter 4

INELASTIC SCATTERING $(3/2^- \rightarrow 1/2^-)$ OF ^7Li

4.1 Introduction

In Chapter 3 (Table 3.1) it was shown that the probability of excitation of ^7Li to its first excited state converges to the value of 6.03×10^{-3}. This is slightly larger than the experimental value of $(5.27 \pm 0.05) \times 10^{-3}$ (Vermeer *et al*, 1984). This discrepancy, although small, should be considered carefully for the following reasons:

1) The experimental value is the ratio of the area of the inelastic peak to the sum of the areas of the elastic and the inelastic peaks and is accurate to within 1%.

2) The $B(E2)$ value calculated by the SCM $(7.4 \pm 0.3e^2fm^4)$ and that extracted from this data $(7.42 \pm 0.14e^2fm^4)$ are in excellent agreement. As mentioned before the difference between the measured values of the $B(E2)$ is due to the model used to treat the continuum states. If the proposed method to treat the continuum states is correctly predicting the E1 effects, then the data should be as closely reproduced as the $B(E2)$ value.

So far only the E1 transitions to the $1/2^+$ continuum states have been included in the calculations. There are of course other E1 transitions that might occur and also the the second order E2 transitions might have an effect on the total contribution from the virtual excitation. Therefore it may be rewarding to look for improvement of calculated values by considering other second order transitions. The transitions that might affect these calculations are :

1) E1 transitions to higher continuum states i.e. $3/2^+$ and $5/2^+$ (L=2) states.

2) E2 transitions to $5/2^-$ and $7/2^-$ (L=3) resonance states.

3) E1 transitions to the virtual excited states of the α particle.

4) E1 transitions to the virtual excited states of triton.

4.2 Other Transitions

4.2.1 L=2 Continuum States

the $3/2^+$ states have smaller effects than $1/2^+$ states and their typical wavefunctions (Figure 4.1) demonstrates this point. The position of the first peak relative to that of the bound state wavefunction results in cancellation in radial integrals. Nevertheless their wavefunctions and corresponding reduced matrix elements are calculated. The total number of continuum states included in the calculation is now 14. The calculated excitation probability corresponding to all the possible transitions between the two bound states and the 14 continuum states is shown in Table 4.1. It should be noted that the E2 transitions between the $3/2^+$ states was also included but did not affect the result.

There is no coupling between $5/2^+$ and $1/2^-$ states and the only possible transitions involving these states are $3/2^- \rightarrow 5/2^+ \rightarrow 3/2^-$ which does not affect the excitation of $1/2^-$ state to the lowest order.

4.2.2 Resonance States

The $7/2^-$ and $5/2^-$ resonance states are also expected to have negligible effects since there is no coupling between $7/2^-$ and $1/2^-$ states and the possible transition $3/2^- \rightarrow 5/2^- \rightarrow 1/2^-$ is a double E2 transition and therefore much weaker than a double E1. This is confirmed by calculation and the results are shown in Table 4.1.

4.2.3 Virtual Excitation of α particle

The virtual states of the $\alpha^* + t$ system are at energies near E_c, the energy cut off of continuum states (Section 3.3), and hence the effect may be very small but it is interesting to study such excitations and their effects. There is no experimental evidence for a bound excited state of the α particle but its first set of excited states, 0^+, 2^+, 1^- are reported between 20–30 MeV (Fiarman and Meyerhof, 1973). The excited state relevant to these calculations, i.e. $\Delta L = 1$, is $J^\pi = 1^-$ at 23.4 MeV. As a first estimate of effects of these excitations, harmonic oscillator wavefunctions are used to calculate the transition matrix elements. The 1^- state couples to triton spin, $1/2^+$, and gives $J^\pi = 3/2^-,\ 1/2^-$. These in turn couple to relative orbital angular momentum , L=1^-, and lead to a triplet $J^\pi = 5/2^+,\ 3/2^+,\ 1/2^+$ around 23.4 MeV and a doublet $J^\pi = 3/2^+,\ 1/2^+$ with centroid at 23.787 MeV. These energy levels correspond to spin–orbit splitting which is assumed to be the same as for the ground state doublet. But the only transitions allowed by angular momentum rules are between the ground state ($J^\pi = 3/2^-$) and the triplet ($J^\pi = 5/2^+,\ 3/2^+,\ 1/2^+$) or between the first excited state ($J^\pi = 1/2^-$) and the doublet ($J^\pi = 3/2^+,\ 1/2^+$). Hence

there are no direct transitions coupling the ground state and the $1/2^-$ state via these continuum states. The only possible transitions are of the form $3/2^- \rightarrow 3/2^+(23.4MeV) \rightarrow 3/2^+(23.787MeV) \rightarrow 1/2^-$ etc. but the matrix elements are large and the overall results on the probability of excitation $(3/2^- \rightarrow 1/2^-)$ could be significant. The transition matrix elements, calculated from the simple harmonic oscillator wavefunction, were also checked by electromagnetic sum rules involving matrix elements (Messiah, 1965)

$$\sum_{J'} \frac{|< J'\|\mathcal{M}_1\|J >|^2}{2J+1} = \frac{|< I_1'\|\mathcal{M}_1\|I_1 >|^2}{2I_1+1}$$

where I_1 is the spin of the excited state (3/2 or 1/2). The final results of including these continuum states are negligible as shown in Table 4.1.

4.2.4 Virtual Excitation of Triton

The virtual excitation of triton can be treated in the same way as that of the α particle. The coupling schemes are different because the spin of the α particle is zero. The excited states of triton are $J^\pi = 3/2^-,\ 1/2^-$ and are coupled to the relative angular momentum which results in a triplet $J^\pi = 3/2^+,\ 3/2^+,\ 1/2^+$ and a doublet $J^\pi = 3/2^+,\ 1/2^+$ with the same splitting as the ground state doublet (0.478 MeV). The existence of excited states of the triton is not experimentally established in a clear way but the measured root mean square radius can be used to estimate an energy $(= \hbar\omega)$ for these states. Using $r_{r.m.s.} = 1.7 \pm 0.05$ fm (Fiarman and Hanna, 1975) the excited state energy will be 21.47 MeV, that is a triplet around 21.47 MeV and a doublet with centroid at 21.948 MeV. These estimates are sufficient for preliminary calculations of the effect of E1 transitions to the continuum states of $\alpha + t^*$ system. In this coupling scheme

all the transitions are allowed except for $1/2^- \rightarrow 5/2^+$. The calculated matrix elements are again checked with electromagnetic sum rules and then included in the calculation of the excitation probability. The results are shown in Table 4.1.

$10^3 \times p_{Coul}$	Transitions
6.389	E2($1/2^-$)
6.030	E2($1/2^-$)+E1($1/2^+$)
5.994	E2($1/2^-$)+E1($1/2^+ + 3/2^+$)
6.021	E2($1/2^-$)+E1($1/2^+$)+E2($5/2^-$ Res)
6.027	E2($1/2^-$)+E1($1/2^+$)+E2($7/2^-$ Res)
6.023	E2($1/2^-$)+E1($1/2^+ + \alpha$ excited states)
6.026	E2($1/2^-$)+E1($1/2^+ + t$ excited states)

Table 4.1

Calculated values for $p(3/2^- \rightarrow 1/2^-)$ with various transitions included. The terms in brackets indicate the states involved in the transition.

4.2.5 Results

It is evident from Table 4.1 that the important effect of E1 transitions come only from $1/2^+(l = 0)$ and $3/2^+(l = 2)$ continuum states of $\alpha + t$ system. All the other effects contribute to a reduction in $p(3/2^- \rightarrow 1/2^-)$ which is far less than the reduction caused by $3/2^+$ states. It should be noted that transitions between the excited states are also possible. That is E2 transitions between $1/2^+$ and $3/2^+$ states or between the $3/2^+$ states themselves could occur. But the inclusion of these transitions in the calculations did not affect the final probability.

Having considered the possible break up states of $\alpha+t$ system, only the $1/2^+$ states ($l = 0$) and the $3/2^+$ states ($l = 2$) are used to calculate the excitation

probability for a range of available data on the inelastic scattering of ^7Li. A box radius of 20 fm and an energy cut off of 20 MeV produce 7 states with $J^\pi = 1/2^+$, the lowest being at 3.138 MeV, and 7 states $J^\pi = 3/2^+$, the lowest being at 3.711 MeV (Figure 4.2).

4.3 Comparison with Data

4.3.1 Data from Vermeer *et al* (1984)

COULVAR is run for all the data points used in the experiment by the Australian group. To compare the results, the ratio p_{exp}/p_{Coul} is calculated and plotted against s, the distance of closest approach of the nuclear surfaces, defined (Fewell *et al*, 1979) as

$$s = a[1 + cosec(\theta/2)] - 1.25[A_1^{1/3} + A_2^{1/3}]$$

where a is the Coulomb parameter (equation 2.26) and θ is the scattering angle; both in the centre of mass system. There are 3 sets of measurements: scattering of ^7Li from ^{208}Pb at 90° for bombarding energies 18–30 MeV, and at 171° for bombarding energies 16–28 MeV and also from ^{138}Ba at 171° and bombarding energies 12.5–21.5 MeV. The results (Figure 4.3) show that these calculations reproduce the shape of p_{exp}/p_{Coul} for all the data. But the ratio p_{exp}/p_{Coul} is around 0.9 as compared to their ratio which is around 1. In the region of $s > 7$ fm the experiment is a pure Coulomb excitation process. That is for these bombarding energies (< 24 MeV for 90°, < 21 MeV for 171° and < 15.5 MeV for Ba) the projectile and the target are always sufficiently far apart that the nuclear forces do not interfere at all. Therefore a good agreement, i.e. $p_{exp}/p_{Coul} \simeq 1$

is expected if the model calculations are to be reliable. Since the $B(E2)$ values are in excellent agreement and also the shape is very well reproduced one can conclude that the destructive E1 interference is present but that the matrix elements are too small. This leads to an underestimate of E1 transition effects and hence a larger p_{Coul}.

This may be due to the ^7Li cluster model since the E1 transition matrix elements are very sensitive to the even parity potentials. These potentials are determined by fitting the phase shift over a limited energy range but the phase shifts are adequately represented via a single parameter, namely the scattering length. Therefore these fits can only determine one parameter. In the SCM calculations the shape of the potential is being kept fixed and the depth is varied to fit the phase shifts. But there is no reason to suppose that the shape is parity independent and RGM (Resonating Group Method) calculations imply that in fact the shape and the depth are both parity dependent. Also the matrix elements strongly depend on the shape of the potential as they involve interference effects. Hence if both the shape and the depth of the nuclear potential were varied one might be able to produce the same phase shift fit with a deeper potential than the one used, at present, for the even parity states. For example if the depth, $V = 70.989$ MeV, used in SCM is replaced by $V = 85$ MeV which is less than the depth of the odd parity potentials, then the resulting matrix elements are large enough to produce an excellent fit to data, for p_{exp}/p_{Coul}, below the Coulomb barrier, as shown in Figures 4.4– 4.6.

4.3.2 Data from Häusser *et al* (1973)

The method is applied to calculate the probability of excitation of ^7Li for these earlier data. This experiment was performed to measure the second order effects, $Q_{3/2^-}$, and the virtual excitation, by scattering ^7Li from ^{208}Pb target at two different scattering angles. In fact a fixed Q value (–3.66 efm^2) was used in the analysis and the best fit values of $B(E2)$ and E1 interference effects were extracted. But the extracted $B(E2)$ value (8.3 ± 0.6) is large since the virtual excitation via the continuum states were treated on the basis of a hydrodynamic model as mentioned in Chapter 3. However the calculations on the basis of the Simple Cluster Model and the E1 transition matrix elements calculated above, result in a very good fit below the Coulomb barrier for both the scattering angles (Figure 4.7).

4.3.3 Data from Bamberger *et al* (1972)

This experiment was the first attempt to measure the quadrupole moment and the effect of virtual excitation, but the results were not accurate enough to extract any reliable value. A good fit was obtained by using a smaller $B(E2)$, i.e. $7.4 \pm 0.1 e^2 fm^4$, which corresponds to including large E1 interference. The E1 effects were calculated on the basis of the continuum states of the $\alpha + t$ system (Smilansky *et al*, 1972). The $Q_{3/2^-}$ value was then extracted using these calculated effects. They obtained a smaller value (-1.0 ± 2.0 e fm^2) compared to the other measurements. As it is shown in Figure 4.8 these data are also well reproduced, below the Coulomb barrier, using the above method for continuum states of SCM.

4.4 Conclusions

Comparison with various data shows that the method devised to calculate the effects of E1 transitions to the breakup states of ^7Li is reliable and can reproduce all the data below the Coulomb barrier, successfully. A good agreement between the calculations and the Australian data was expected on the basis of corresponding $B(E2)$ values. But the consistent agreement with other data confirms the fact that the discrepancy between $B(E2)$ values is indeed due to the different treatments of E1 transition effects. It also shows that the proposed method for treating the continuum states is a reliable method for determining such effects.

This is very encouraging as the method can be used to test nuclear models by fitting Coulomb excitation data. For example the problem of the even parity potentials which is really connected to the SCM model, not the method used to treat the continuum states, may be solved by the application of the proposed method. The potential parameters of SCM can be adjusted to produce the required matrix elements to fit the Coulomb excitation data as well as other properties of ^7Li, simultaneously. Hence the even parity potentials can be determined uniquely

The region of $s < 8$ fm in figure 4.2 corresponds to the incident energies large enough for the interference of the nuclear forces. Hence a pure Coulomb excitation calculation is not a valid approximation. This interference may be treated approximately as a correction to the Coulomb interaction, i.e. retaining the Coulomb orbits. This is discussed in the following Chapter.

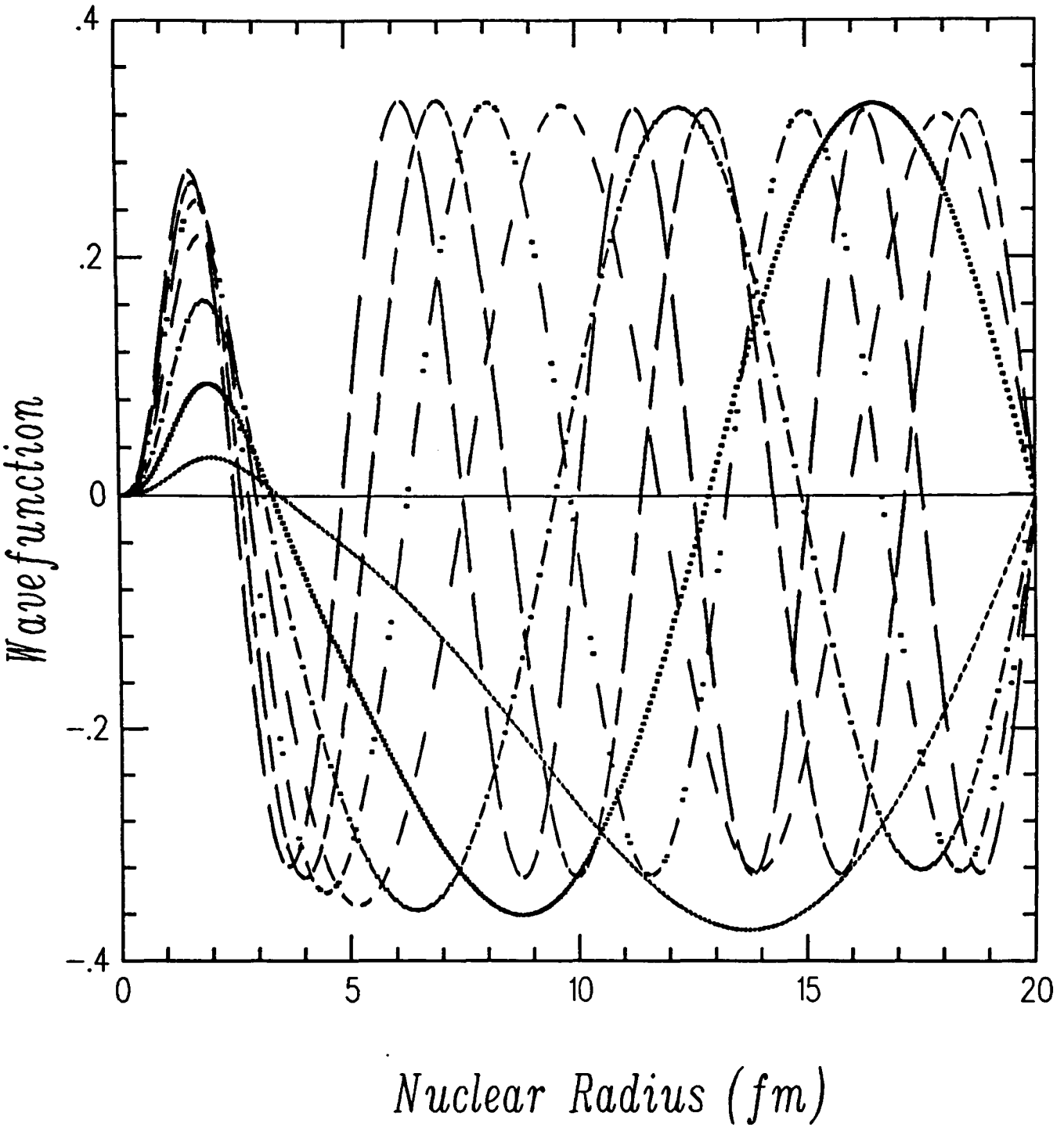

Figure 4.1

Wavefunctions of $3/2^+$ continuum states. The box radius is 20 fm and the cut off energy is 20 MeV. The ground state wavefunction is negligible for $r > 7$ fm (Figure 3.2).

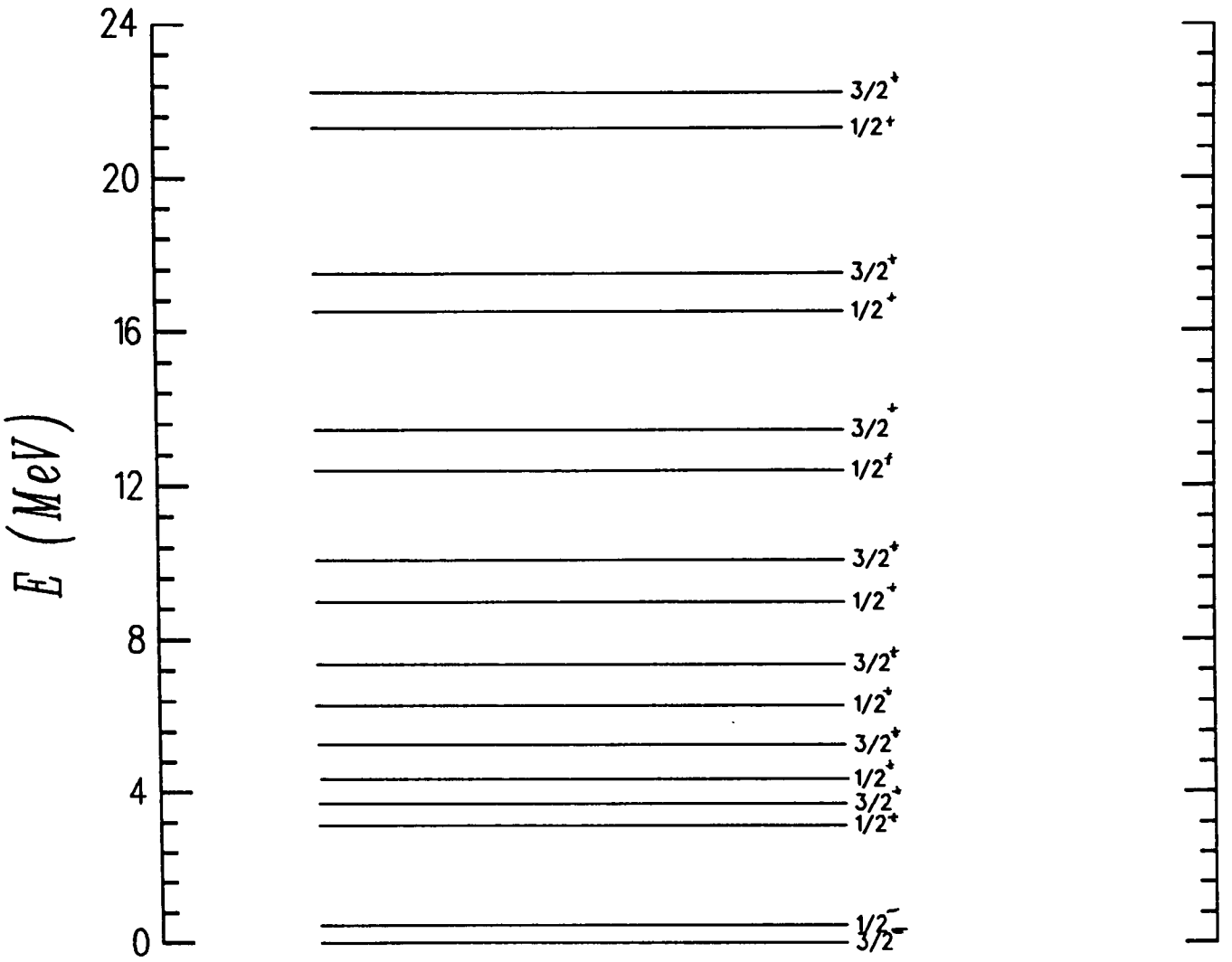

Figure 4.2

Energy levels of ^7Li, used in the calculation of $P(3/2^- \rightarrow 1/2^-)$.

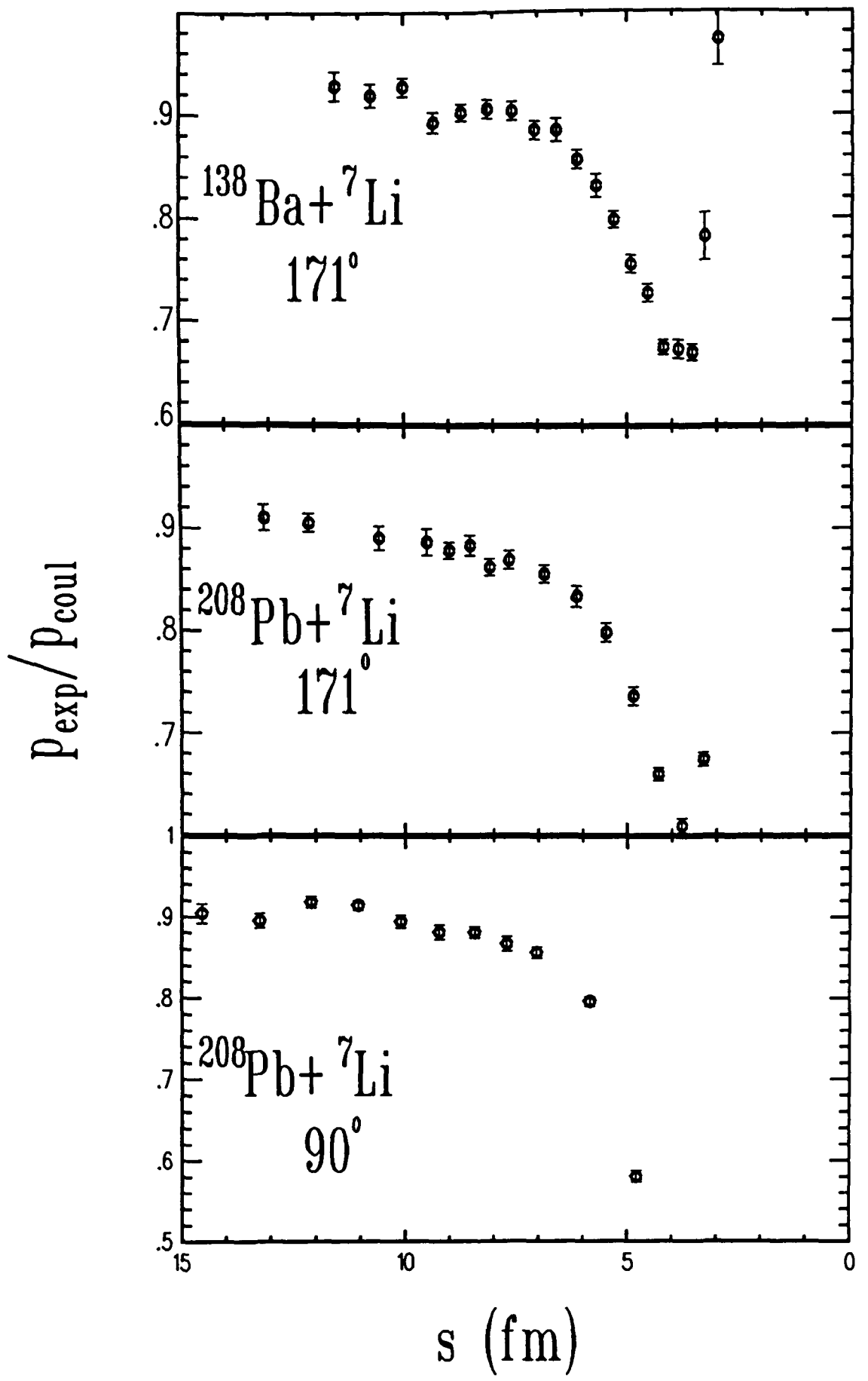

Figure 4.3

Probability of excitation ($3/2^- \rightarrow 1/2^-$) of ^7Li for various cases. P_{exp} is the experimental result, p_{Coul} is the calculated probability and s is the distance of closest approach of nuclear surfaces.

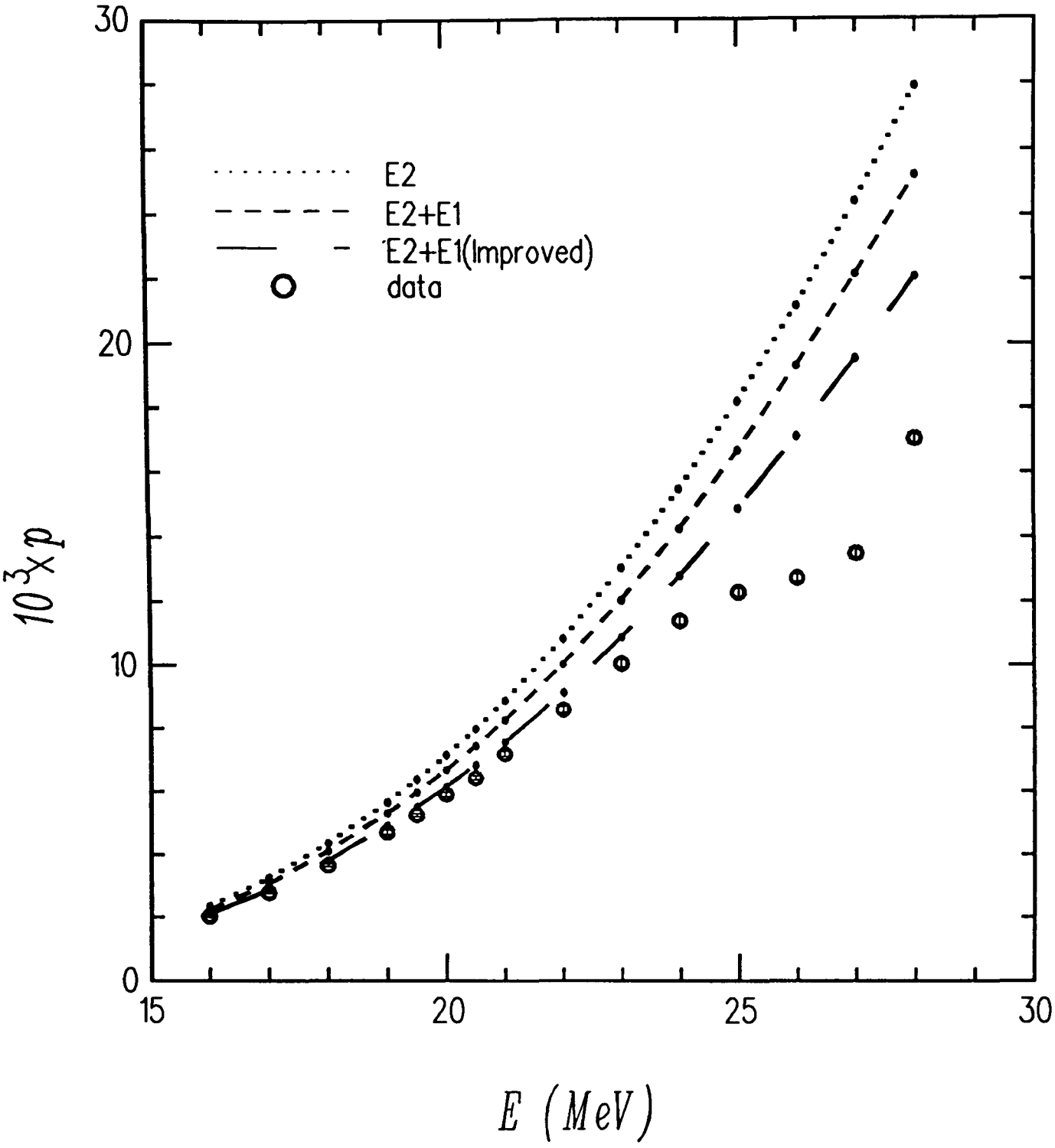

Figure 4.4

$p(3/2^- \rightarrow 1/2^-)$ for $^7Li +^{208} Pb$ at 171°. E is the lab energy. Improved calculations are obtained by using the matrix elements calculated with a deeper potential for s states.

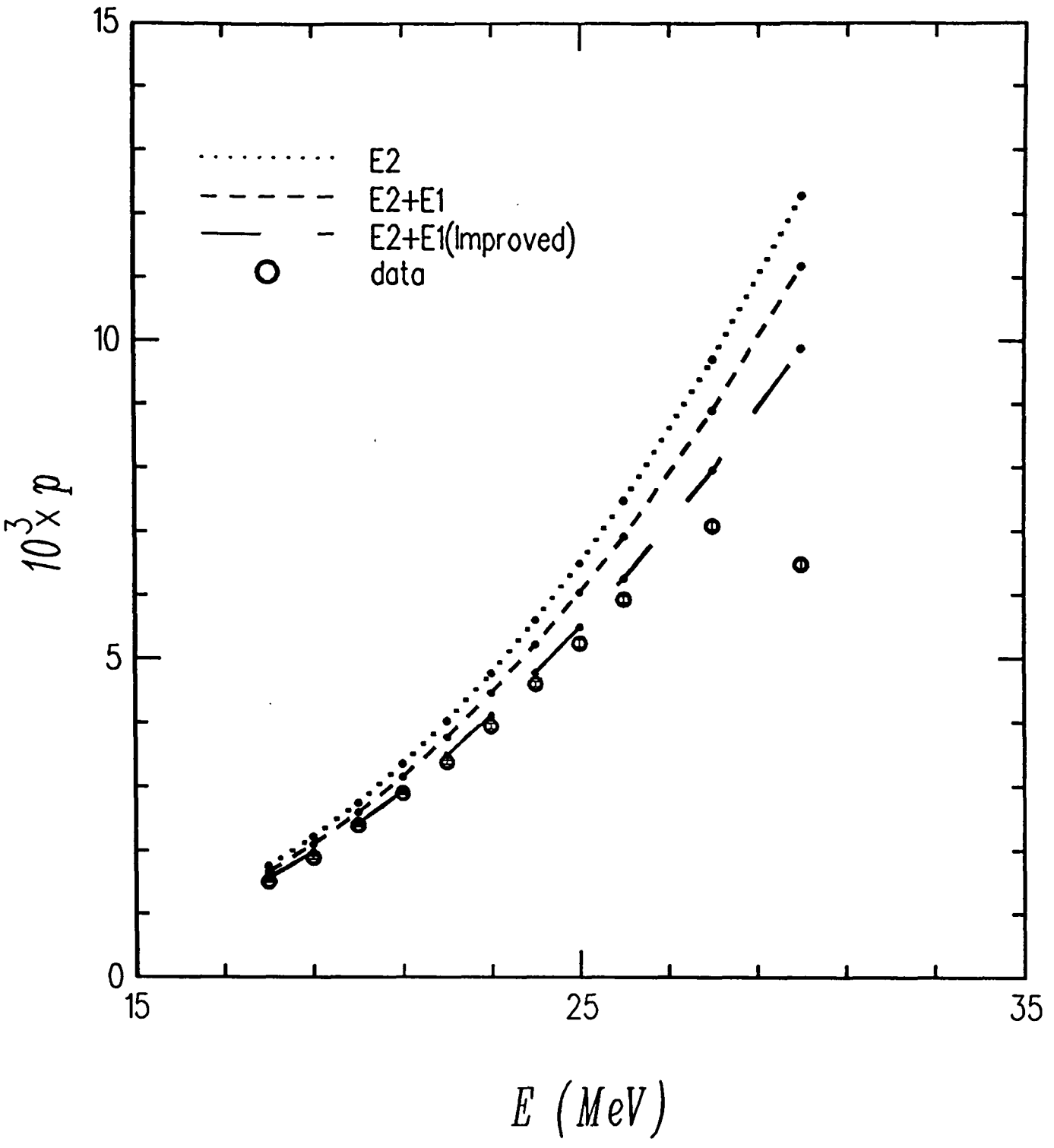

Figure 4.5

$p(3/2^- \rightarrow 1/2^-)$ for $^7Li +^{208} Pb$ at 90°. E is the lab energy. Improved calculations are obtained by using the matrix elements calculated with a deeper potential for s states.

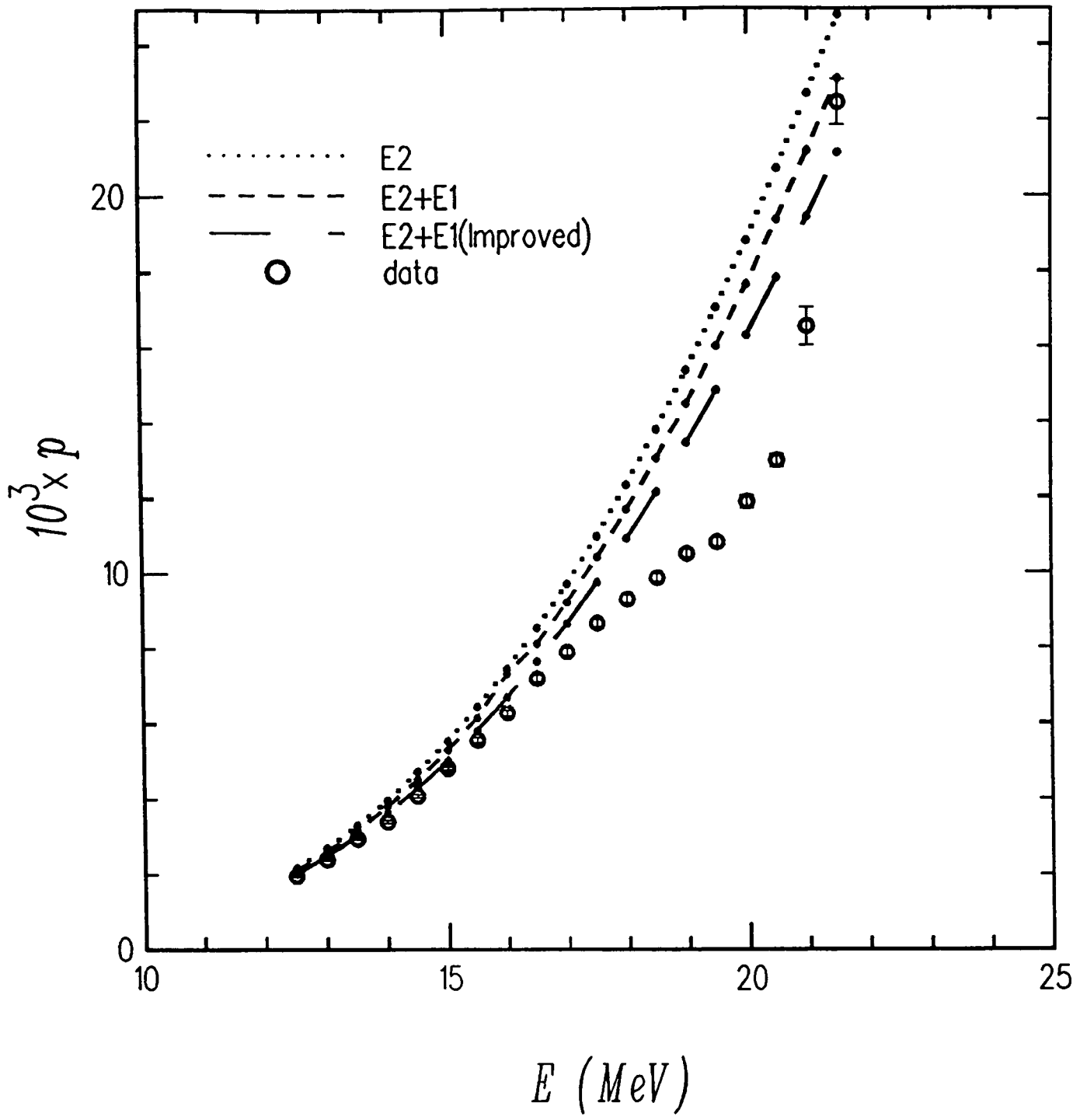

Figure 4.6

$p(3/2^- \rightarrow 1/2^-)$ for $^7Li + ^{138}Ba$ at 171°. E is the lab energy. Improved calculations are obtained by using the matrix elements calculated with a deeper potential for s states.

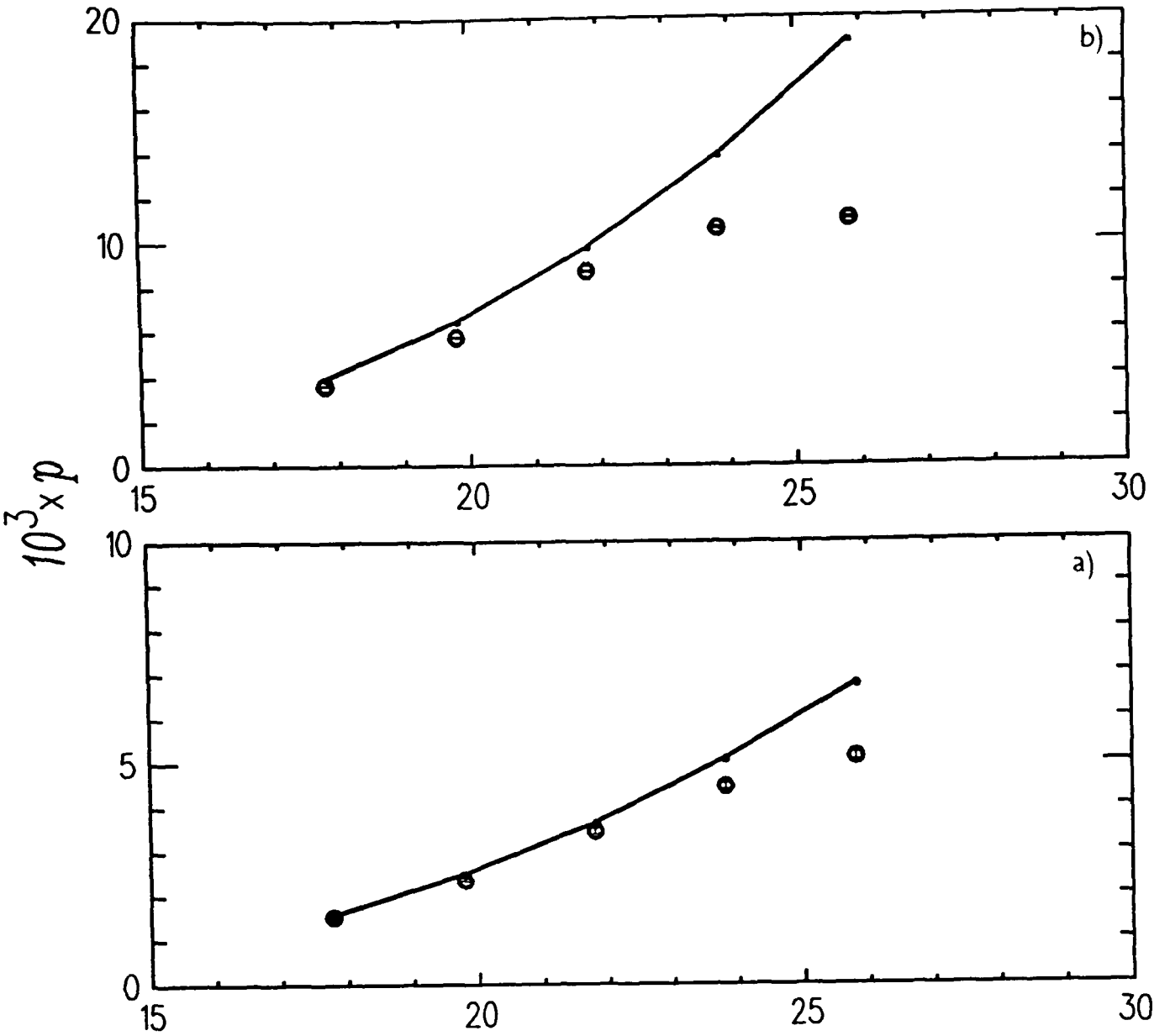

Figure 4.7

Probability of excitation ($3/2^- \rightarrow 1/2^-$)of ^7Li at 173° (**a**) and 90° (**b**). . E is the lab energy and data is from Häusser *et al.*

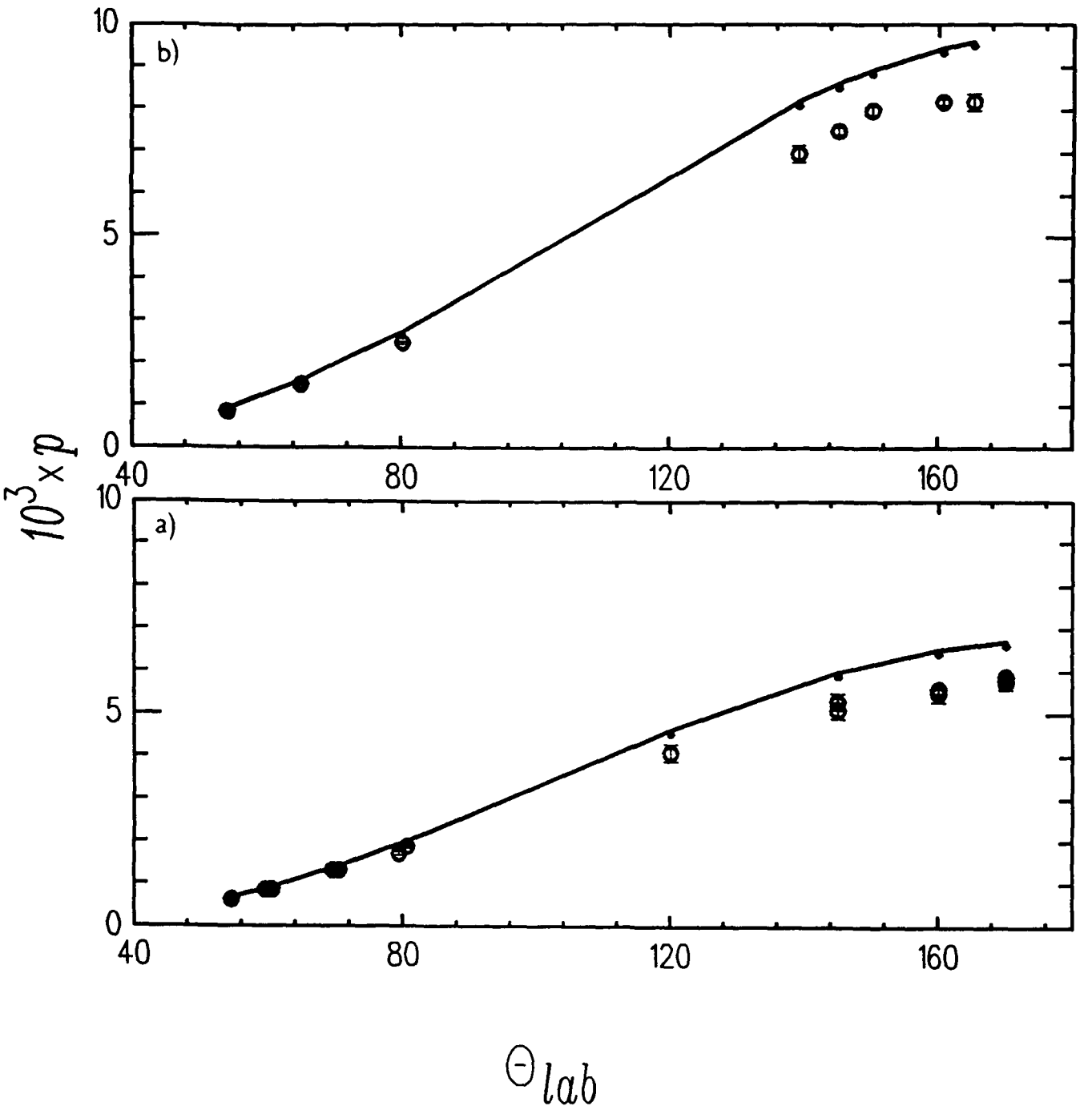

Figure 4.8

Probability of excitation ($3/2^- \rightarrow 1/2^-$) of ^7Li at 22 MeV (**a**) and 20 MeV (**b**). Data from Bamberger *et al.*

Chapter 5

COULOMB–NUCLEAR INTERFERENCE

5.1 Introduction

In this chapter the Coulomb–nuclear interference at the sub–barrier energies is treated. In Chapter 3 it was mentioned that the sudden deviation of calculated $p(3/2^- \rightarrow 1/2^-)$ from the measured one is due to the interference of the short range nuclear interaction. As seen in Figures 4.4–4.8, a pure Coulomb excitation calculation results in a rapidly increasing p, whereas the interference of an attractive nuclear interaction with the repulsive Coulomb force results in a gradual increase and the probability becomes almost constant at some point before starting to rise again. This is typical of such interference behaviour. As the nuclei get closer the nuclear forces become stronger and the destructive effects on p are increased, hence the gradual decrease. When the two forces become equal in magnitude then the net force is very small leading to a shoulder. Eventually the magnitude of the nuclear force exceeds that of the Coulomb force and the excitation probability starts to rise again. However the calculations involving nuclear forces are more complicated since they involve rather

more than just integrating along the Coulomb orbit. That is, the assumption of semi–classical method leading to a classical orbit is no longer valid and a full quantum mechanical calculation is required.

The coupled channel calculations for nuclear interactions alone have been performed successfully and there are many computer codes available for such calculations. Recently the Coulomb interaction has also been included in some of these codes but it is only applicable to the nuclei with integer spin ground state, hence it can not be used for ^{7}Li.

However at low energies one may be able to calculate such effects approximately by treating the nuclear interaction as a perturbation to the Coulomb interaction. Since at the sub–barrier energies the Coulomb force is much stronger than the nuclear force one may assume the classical orbit is not disturbed. Then the above approximation is justified and it is possible to include the nuclear interactions in the existing Coulomb excitation codes.

This Chapter covers the details of such a procedure and the results of its application to ^{7}Li. In Section 5.2 the assumptions and mathematical formalism are discussed and the first results are presented in Section 5.3. Section 5.4 is a discussion of possible improvements of these results and their applications. The final conclusions and a summary of the results are presented in Section 5.5.

5.2 Multipole Expansion of Nuclear Interaction

The basic assumption for this method is that the Coulomb orbit is essentially unperturbed but that there is an extra term in the interaction that has to be considered. i.e. equation (2.10) should be replaced by

$$\mathcal{H}_E(t) = V_C + V_n \tag{5.1}$$

where V_n is the nuclear interaction and V_C is the electrostatic potential (Coulomb term). Now, if V_n can be written in terms of a multipole expansion similar to that of V_C, equation (2.13), then it can be easily incorporated into a Coulomb excitation code. The simplest way to achieve such expansion is to find a form of V_n which can be readily expanded.

Near the Coulomb barrier the distance between the nuclei is large compared to the range of nuclear forces. Therefore only the behaviour of the nuclear potential at large radius is important, i.e. only the tail of V_n is involved in such interactions. If one assumes a Woods–Saxon shape for the nuclear potential between the projectile and the target then the effective nuclear potential is given by

$$V_n = V_0 e^{(R_0 - x)/a_0} \tag{5.2}$$

where V_0, R_0 and a are the parameters of the Woods–Saxon potential and x is the distance between the centres of mass of the two nuclei.

The interaction between ^7Li and the target involves a 3-body problem as mentioned before, but the calculations can be simplified by expressing the target–projectile interaction in terms of the individual cluster–target interactions. The latter can then be expressed as a function of relative separation of the clusters and that of the target and projectile. Figure 5.1 illustrates the relation between different interactions.

The cluster–target interaction is spherical i.e.

$$V_\alpha(\mathbf{R}_\alpha) = V_\alpha(R_\alpha)$$

$$V_t(\mathbf{R}_t) = V_t(R_t)$$

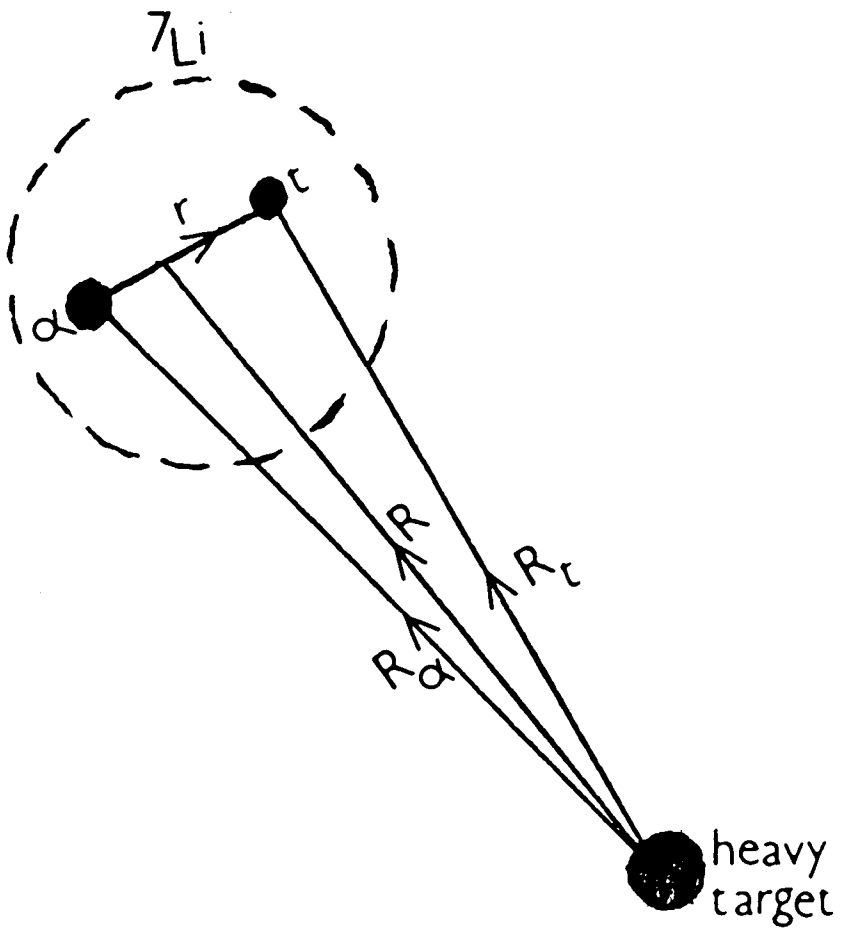

Figure 5.1

The radii for target, projectile and cluster interactions. **r** is the separation between the clusters and **R** is that between the projectile and the target. The distances are between the centres of mass.

From Figure 5.1

$$\begin{aligned} \mathbf{R}_\alpha &= \mathbf{R} - \frac{m_t}{M}\mathbf{r} \\ \mathbf{R}_t &= \mathbf{R} + \frac{m_\alpha}{M}\mathbf{r} \end{aligned} \tag{5.3}$$

Hence the interaction potential can be written as

$$\begin{aligned} V(\mathbf{R},\mathbf{r}) &= V_\alpha(\mathbf{R}_\alpha) + V_t(\mathbf{R}_t) \\ &= V_\alpha(|\mathbf{R} - \frac{m_t}{M}\mathbf{r}|) + (V_t(|\mathbf{R} + \frac{m_\alpha}{M}\mathbf{r}|) \end{aligned} \tag{5.4}$$

where M is the projectile mass i.e. $M = m_\alpha + m_t$. Using the last expression (equation 5.4), the potential of equation 5.2 can be written as

$$\begin{aligned} V(R) &= V_{\alpha 0} e^{(R_{\alpha 0} - |\mathbf{R} - \frac{m_t}{M}\mathbf{r}|)/a_{\alpha 0}} + V_{t0} e^{(R_{t0} - |\mathbf{R} - \frac{m_\alpha}{M}\mathbf{r}|)/a_{t0}} \\ &= [V' e^{-a'|\mathbf{R} - \nu\mathbf{r}|}]_\alpha + [V' e^{-a'|\mathbf{R} - \nu\mathbf{r}|}]_t \end{aligned} \tag{5.5}$$

where $V' = V_0 e^{R_0/a_0}$, $a' = 1/a_0$ and $\nu = m/M$.

Now a multipole expansion for the exponential term, $e^{-a'|\mathbf{R}-\mathbf{r}|}$, is needed. Consider the expansion of the well known Green function $\frac{e^{-ik|\mathbf{R}-\mathbf{r}|}}{|\mathbf{R}-\mathbf{r}|}$ which is given by Merzbacher (1961) as

$$\frac{e^{ik|\mathbf{R}-\mathbf{r}|}}{|\mathbf{R}-\mathbf{r}|} = ik \sum_{lm} h_l^{(1)}(kR) j_l(kr) P_l(\hat{\mathbf{R}}.\hat{\mathbf{r}}) \qquad \text{for } R > r \tag{5.6}$$

Since the cluster separation is small and the projectile–target separation is large one can use the asymptotic behaviour of j and $h^{(1)}$ given (Merzbacher, 1961) by

$$\lim_{x\to\infty} h_l^{(1)}(x) = \frac{e^{i(x-(l+1)\pi/2)}}{x} \quad \text{and} \quad \lim_{x\to 0} j_l(x) = \frac{x^l}{(2l+1)!!} \tag{5.7}$$

Now substituting $\kappa = -ik$ and writing $P_l(\hat{\mathbf{R}}.\hat{\mathbf{r}})$ in terms of the spherical harmonics, equation 5.6 becomes

$$\frac{e^{-\kappa|\mathbf{R}-\mathbf{r}|}}{|\mathbf{R}-\mathbf{r}|} = -4\pi\kappa \sum_{lm} h_l^{(1)}(i\kappa R) j_l(i\kappa r) Y_l^m(\hat{\mathbf{R}}) Y_l^{m*}(\hat{\mathbf{r}}) \tag{5.8}$$

and the asymptotic relations (equation 5.7) become

$$\begin{aligned} \lim_{R\to\infty} h_l^{(1)}(i\kappa r) &= \frac{e^{i(i\kappa R-(l+1)\pi/22)}}{i\kappa R} = \frac{-(-i)^l e^{-\kappa R}}{\kappa R} \\ \text{and} \quad \lim_{r\to 0} j_l(i\kappa r) &= \frac{(i\kappa r)^l}{(2l+1)!!} \end{aligned} \tag{5.9}$$

Using these expressions in equation 5.8 gives

$$\begin{aligned} \frac{e^{-\kappa|\mathbf{R}-\mathbf{r}|}}{|\mathbf{R}-\mathbf{r}|} &\simeq -4\pi\kappa \sum_{lm} -(-i)^l \frac{e^{-\kappa R}}{\kappa R} \frac{(i\kappa r)^l}{(2l+1)!!} Y(\hat{\mathbf{R}}) Y^*(\hat{\mathbf{r}}) \\ &\simeq 4\pi \sum_{lm} \frac{e^{-\kappa R}}{R} \frac{(\kappa.r)^l}{(2l+1)!!} Y(\hat{\mathbf{R}}) Y^*(\hat{\mathbf{r}}) \end{aligned} \tag{5.10}$$

Now noting that

$$\frac{-d}{d\kappa}\left[\frac{e^{-\kappa|\mathbf{R}-\mathbf{r}|}}{|\mathbf{R}-\mathbf{r}|}\right] = e^{-\kappa|\mathbf{R}-\mathbf{r}|}$$

one can differentiate both sides of equation 5.10 with respect to κ to get

$$\begin{aligned} e^{-\kappa|\mathbf{R}-\mathbf{r}|} &= \sum_{lm} \frac{-1}{R(2l+1)!!}(-Re^{-\kappa R}(\kappa r)^l + e^{-\kappa R} l\kappa^{l-1} r^l) Y(\hat{\mathbf{R}}) Y^*(\hat{\mathbf{r}}) \\ &= 4\pi \sum_{lm} \kappa^l e^{-\kappa R} \frac{r^l}{(2l+1)!!}(1 - \frac{l}{R\kappa}) Y(\hat{\mathbf{R}}) Y^*(\hat{\mathbf{r}}) \end{aligned} \tag{5.11}$$

Since $R \gg 1$ then $(1 - l/R\kappa) \simeq 1$ and noting that $r^l Y^*(\hat{\mathbf{r}})$ is time independent and is included in the transition matrix elements of equation (2.15), one can now relate equations (5.11) and (2.16) such that only the integration routine of COULVAR needs to be modified by adding an extra interaction term. If the above expansion (equation 5.11) is used in the expression for V_n (equation 5.5) and then it is added to the interaction term $\mathcal{H}_E(t)$ (equation 2.13), equation (2.16) becomes

$$S_{E\lambda,\mu} = \int_{-\infty}^{+\infty} (\frac{e^{i\omega t}}{r_p^{l+1}(t)} - \frac{V'(\nu a')^\lambda}{(2\lambda-1)!!} e^{-a' r_p(t)}) Y_{\lambda\mu}(\theta_p(t), \phi_p(t)) dt \tag{5.12}$$

where the second term in the bracket is the time dependent part of the nuclear interaction and includes both the α–target and the t–target potentials i.e.

$$F_{nuc}(r_p(t)) = [V' \frac{(a'\nu)^\lambda}{(2\lambda-1)!!} e^{-a' r_p(t)}]_\alpha + [\ \ldots\ldots\ ]_t \tag{5.13}$$

V', a' and ν are defined above (equation 5.5). The negative sign of F_{nuc} in equation 5.12 corresponds to the attractive nuclear interaction as compared to the repulsive Coulomb force.

5.3 Calculations and Results

Since the main interaction in these cases is the quadrupole Coulomb interaction , only the term corresponding to $\lambda = 2$ in the multipole expansion of the nuclear interaction (equation 5.11) is included in the code, i.e.

$$F_{nuc}(r_p(t)) = [V' \frac{(a'\nu)^2}{15} e^{-a' r_p(t)}]_\alpha + [\ \ldots\ldots\ ]_t \tag{5.14}$$

is added to the Coulomb interaction in the integration routine. The parametric forms of r_p and t given by equation (2.19) are used and values of V' and a' are taken from scattering experiments. Ideally one needs the parameters of a Woods–Saxon potential for $\alpha + ^{208}Pb$ and $t + ^{208}Pb$ around 17 and 12 Mev respectively (4/7 and 3/7 of bombarding energy, the highest is 29 MeV for this case). The closest energy range of the available scattering experiments is the scattering at 20 MeV (Perey and Perey, 1976) for both cases.

At first only the parameters of the real Woods–Saxon potential are used and the results are shown in Figures 5.2 and 5.3. It is evident that although the effect of the interference follows the expected shape of the excitation probability it seems to be very strong. Therefore the imaginary potential was also included, using the potential parameters of the same data. The results are also shown in Figures 5.2 and 5.3 and they illustrate the importance of the imaginary part at the short nuclear radii (well above the Coulomb barrier). However it does not seem to affect the values at those energies which are well below the Coulomb barrier. There are two other factors that might improve the results:

1) The assumption of a perturbed Coulomb orbits is not valid and the nuclear orbits should be taken into account,

2) The nuclear potentials fitted by the scattering processes are only fitted for the short nuclear radius and may not be a good fit at these large distances.

These points and their applications are discussed in detail in the following section.

5.4 Improvements of Nuclear Perturbations

The effect of nuclear orbits in such calculations has been studied by Landowne *et al* (1986). They have investigated the inelastic scattering of $^{16}O + ^{208}Pb$ at low energies where the cross sections depend directly on the Coulomb–nuclear interference. They show that if the Woods–Saxon potential for $E = 104$ MeV is used then the nuclear coupling is underpredicted but, larger nuclear form factors (almost twice as strong) provide a very good fit to the data. This is related to the second improvement suggested above, but the important point is that when these form factors are used with pure Coulomb waves the results are almost the same. It is interesting to note that they also show that the strength of the imaginary potential is irrelevant for low energy excitation, as mentioned above. Furthermore the inverse scattering calculations by Mackintosh and his collaborators (detailed below) provide strong evidence supporting the second suggestion above, namely the refitting of the nuclear potentials.

Calculations of model independent fits to ^{6}Li data (Mackintosh and Kobos, 1982) suggest that the ^{6}Li real potential should be smaller than the folding model and that this renormalisation can indeed be attributed to the break up effects. Further studies of $^{6}Li + ^{12}C$ at 156 MeV (Ioannides and Mackintosh, 1986) show that the real potential is decreased by 50–60% in the surface region but the imaginary potential is relatively unaffected by the break up. But the calculations for ^{16}O on ^{208}Pb near or below the Coulomb barrier (Ioannides and Mackintosh, 1985) suggest a highly attractive potential in the surface since the potential is increased by some 80% in a significant part of the surface region.

They have not been able, as yet, to perform inversion calculations for half integer spin particles so no specific conclusions can be drawn for ^{7}Li. But it is suggested (Mackintosh, 1987) that the result of $^{16}O +^{208} Pb$ calculation at low energies is more relevant to the inelastic scattering of ^{7}Li than the high energy ^{6}Li results. The assumption behind all these calculations is that when break up is included in the inelastic scattering calculations then such renormalised potentials should be used. On the basis of these results and those of Landowne *et al* it seems more reasonable to consider the refitting of the potentials rather than the recalculation of the orbits.

The refitted potentials may be obtained by varying the potential parameters such that the Coulomb excitation results are fitted to the data. The form of the potential $V_0 e^{(R_0-x)/a_0)}$ (equation 5.2) shows that there are only two effective parameters. Furthermore the effects of the variation of V_0 and a_0 show that the important factor is a_0. Only a small change in $p(3/2 \rightarrow 1/2)$ is obtained by a large increase in V_0 whereas a small change in a_0 results in a sizeable change in p. Therefore a_0 for both α and t real potentials is varied to get the best fit results for Coulomb scattering data. Figure 5.4 shows the results of such fitting for the case of $^{7}Li +^{208} Pb$ scattering at an angle of 171°. An excellent fit is obtained by increasing $a_{0\alpha}$ from 0.625 fm to 1.1 fm and a_{0t} from 0.795 fm to 1.05 fm. A similarly good fit is obtained for the case of a 90 degree scattering angle (Figure 5.5). it should be noted that the the last point of this data is close to the Coulomb barrier and the nuclear force may be strong enough to deflect the orbit.

5.5 Conclusions

The final result of these calculations is very interesting and also encouraging. It is interesting since it suggests a unique way of determining the behaviour of the nuclear potentials at large distances. That is the Coulomb scattering data can be used to fit the nuclear potential at large nuclear radii. It should be clearly emphasised that these fitted parameters are only valid for large nuclear radii and are complementary to the parameters determined from the nuclear scattering processes at short range. In fact most nuclear scattering experiments only determine the nuclear potential for small radii, and do not give much information about the behaviour at large radii. Using the Coulomb scattering data the large distance behaviour may also be determined and then a more realistic potential over a greater range is obtained.

The fact that the model for continuum states is capable of coping with more approximations is encouraging for the stability of the model. Although the Coulomb-nuclear interference does not depend on the model for continuum states the Coulomb scattering data can only determine the large distance potential if the calculated excitation probabilities are known as accurately as possible. Therefore it is important to have a model which correctly predicts the E1 effects and the excitation probabilities in the region of pure Coulomb excitation.

It is also interesting to note that the behaviour of fitted potentials seems to agree with the results of inverse scattering calculations. That is the potentials (Figure 5.6) are more attractive in the surface region. This agreement and the

good fits of Figures 5.3 and 5.4 are reasonable enough to justify the choice of refitting the potentials rather than recalculating the nuclear effects on the orbits.

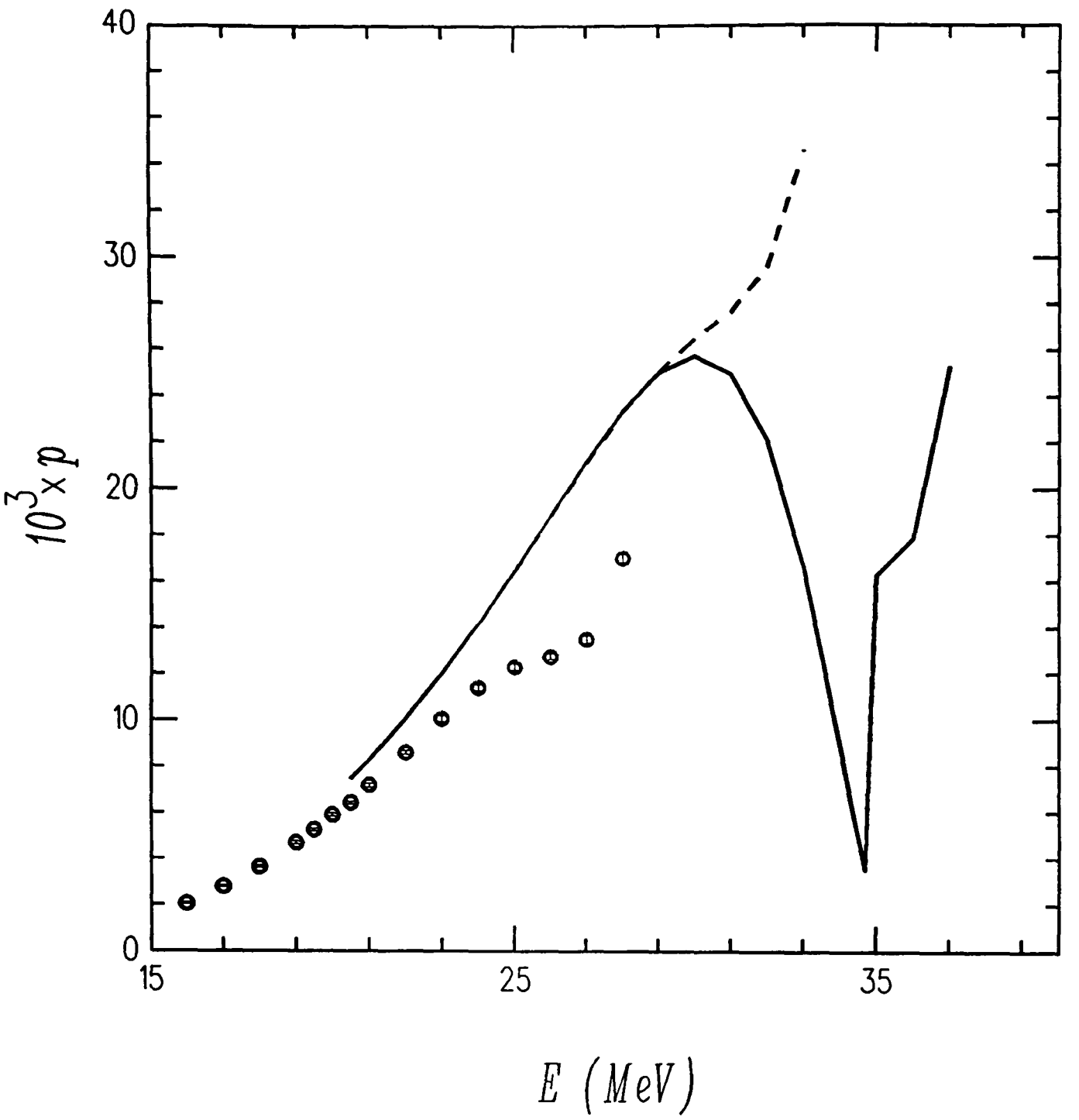

Figure 5.2

The effect of nuclear potential on the probability of excitation ($3/2^- \rightarrow 1/2^-$) of ^7Li. The solid line corresponds to the real part only and the dashed line to the real and imaginary part. Data is from Vermeer *et al*, target is ^{208}Pb and the scattering angle is 171°.

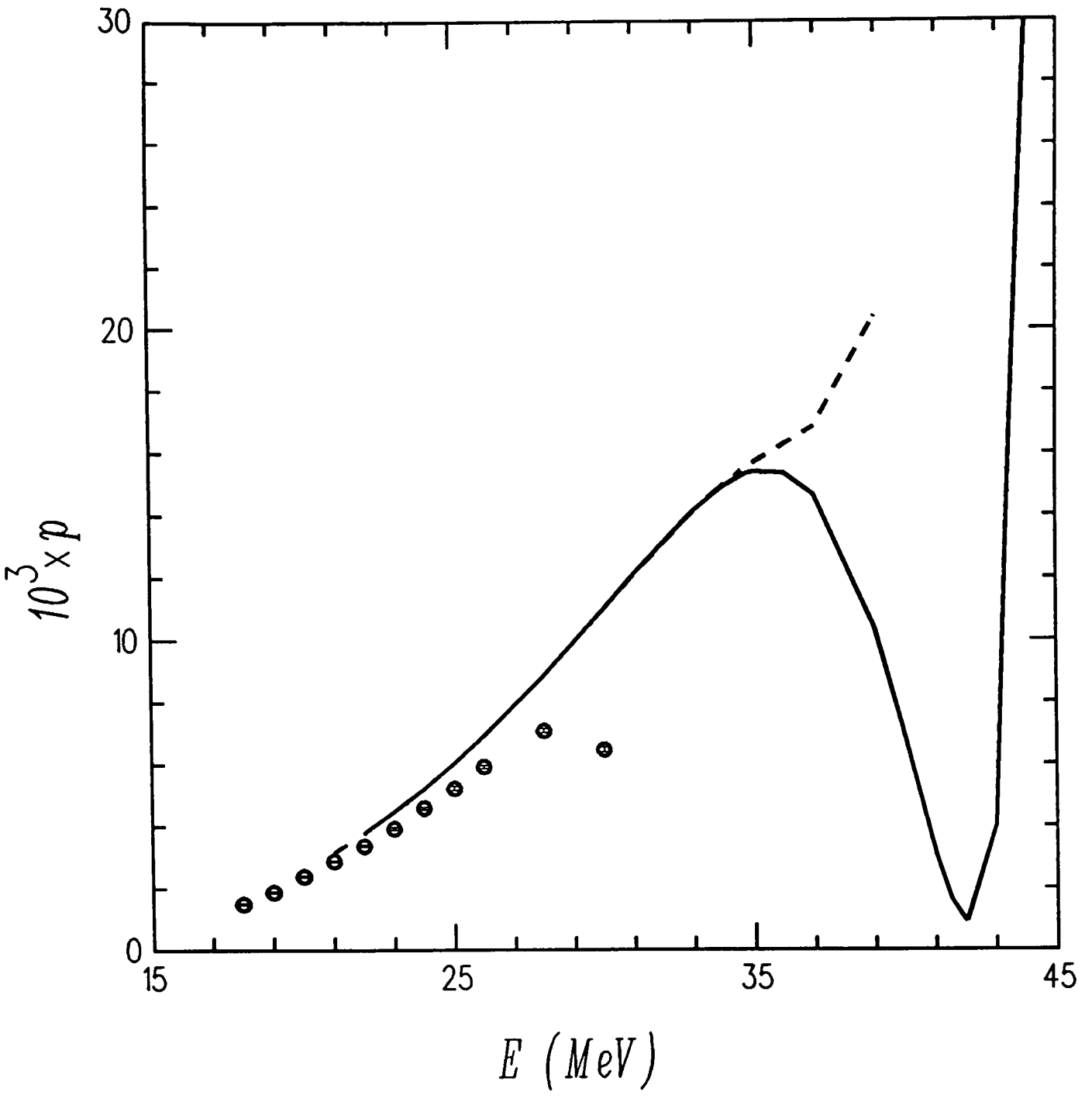

Figure 5.3

The effect of nuclear potential on the probability of excitation ($3/2^- \rightarrow 1/2^-$) of ^7Li. The solid line corresponds to the real part only and the dashed line to the real and imaginary part. Data is from Vermeer *et al*, target is ^{208}Pb and the scattering angle is 90°.

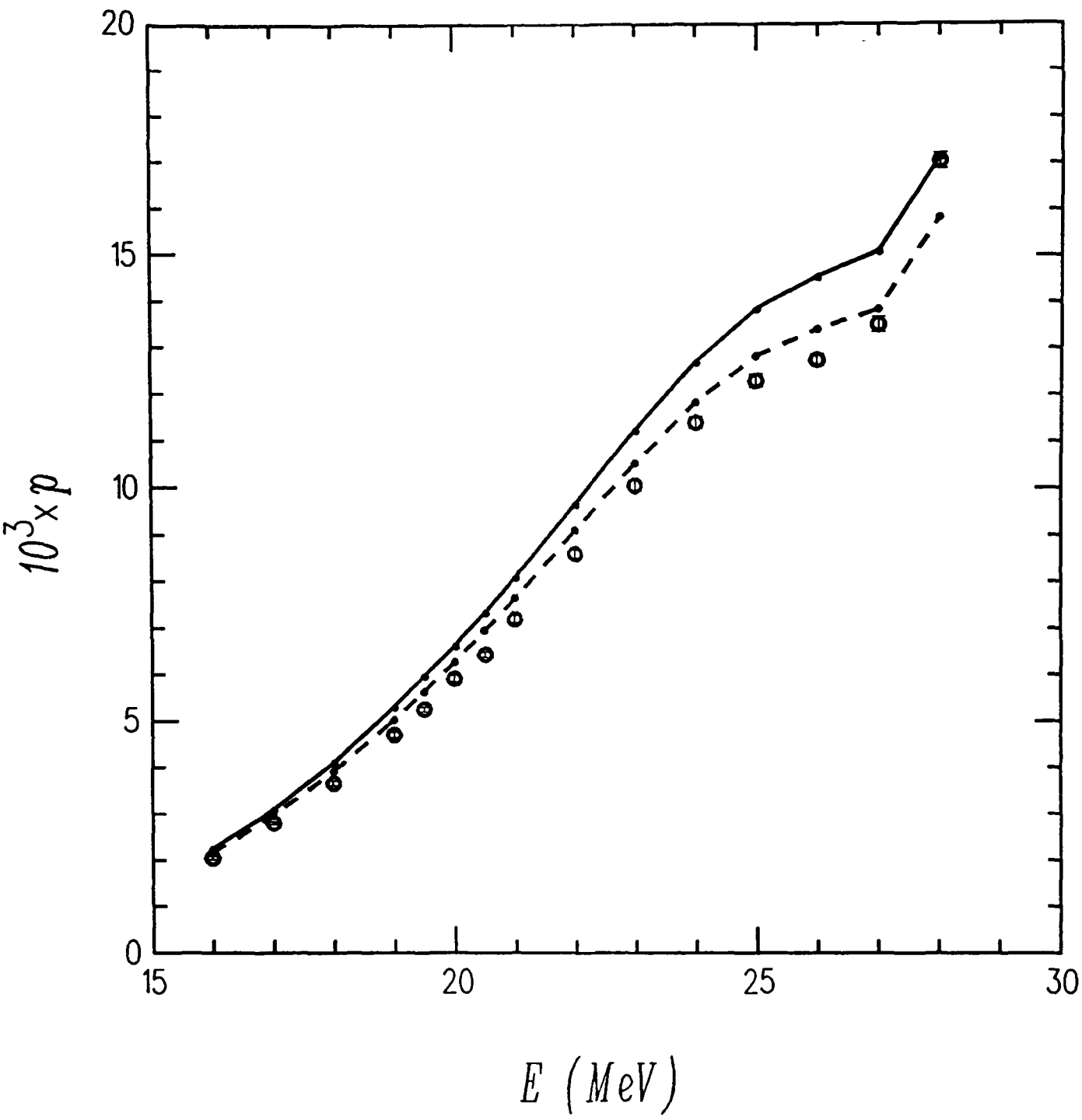

Figure 5.4

Probability of excitation ($3/2^- \rightarrow 1/2^-$) of ^7Li calculated with fitted nuclear potential. Data is from Vermeer *et al* for $^7Li + ^{208}Pb$ at the scattering angle of 171 °. The dashed line is obtained using the larger matrix elements (see 4.3.1).

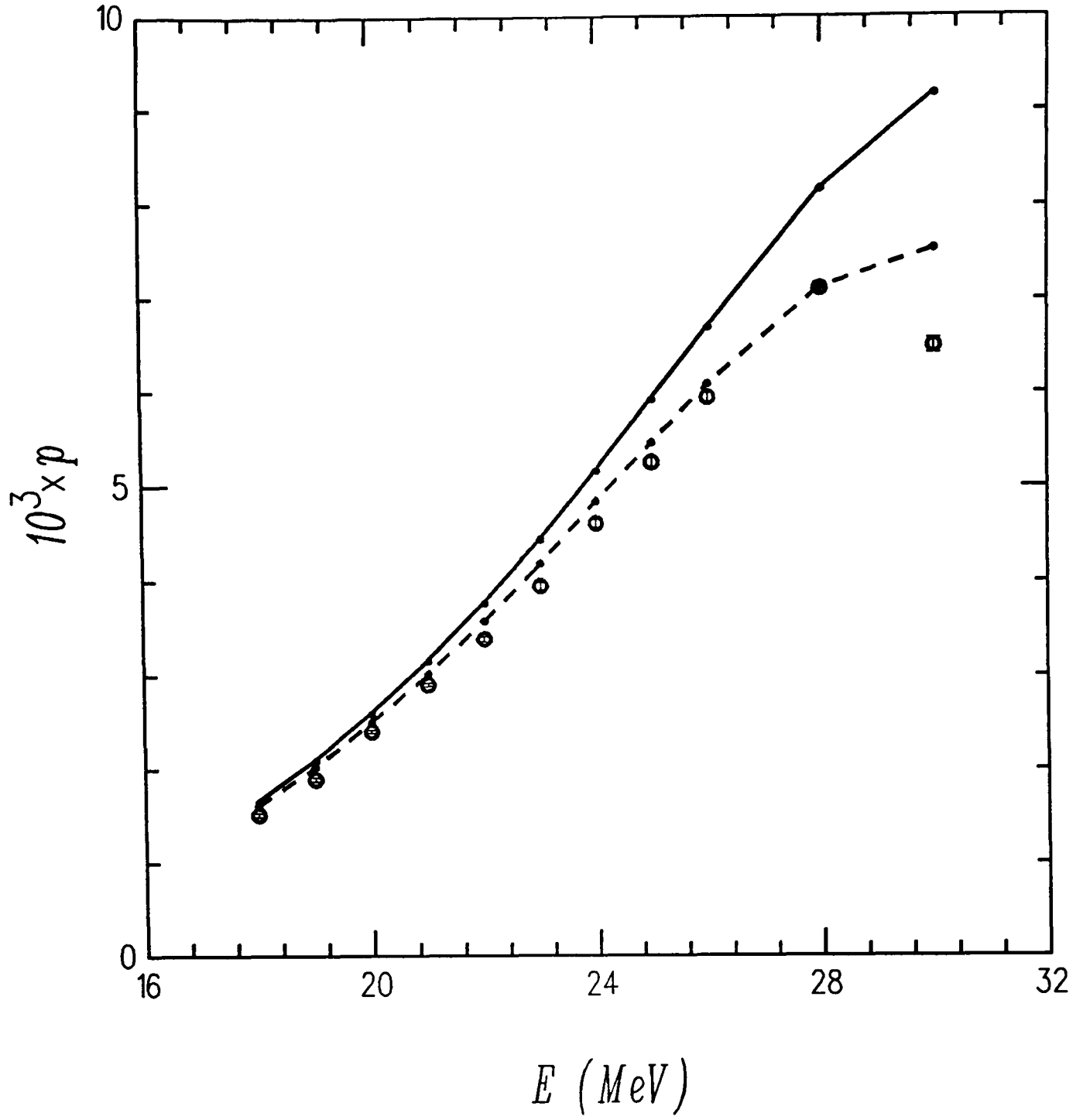

Figure 5.5

Probability of excitation ($3/2^- \rightarrow 1/2^-$) of ^7Li calculated with fitted nuclear potential. Data is from Vermeer *et al* for $^7Li + ^{208}Pb$ at the scattering angle of 90°. the dashed line is obtained using the larger matrix elements (see 4.3.1).

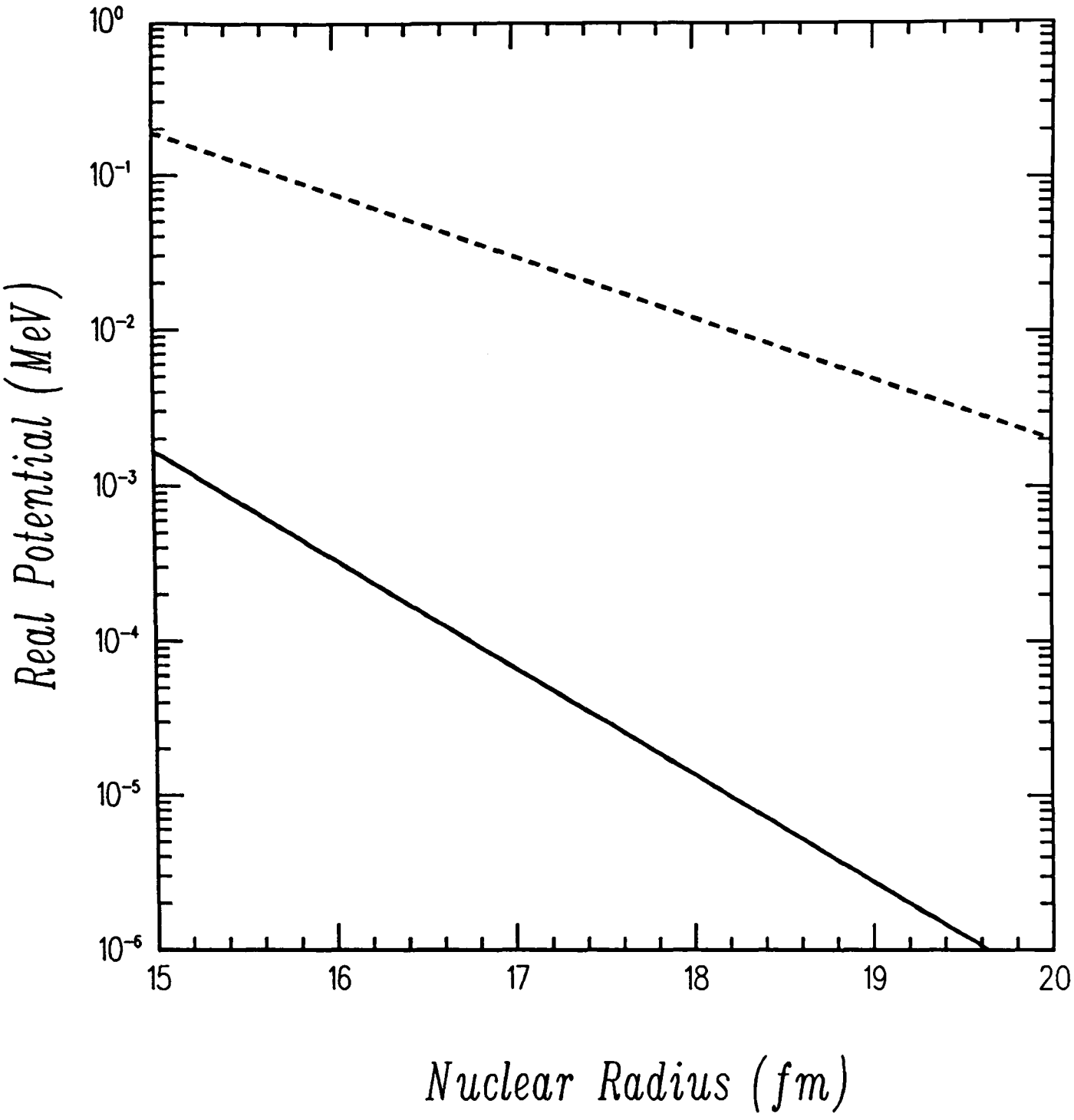

Figure 5.6

The modulus of the tail of the α–^{208}Pb nuclear potential is plotted. The solid line represents the scattering potential and the dashed line represents the potential fitted to the Coulomb excitation data.

Chapter 6

COULOMB BREAK UP OF ^7Li

6.1 Introduction

Coulomb break up is the term used for fragmentation of a nucleus under the influence of the Coulomb force. Although Coulomb excitation occurs at low energies (below the Coulomb barrier) if the projectile is excited to the states above the break up threshold which have small energy widths, then the projectile may sequentially break up. On the other hand at high energies the nucleus may undergo a rapid fragmentation in the surface field of the target. That is, it breaks up at large nuclear radius where the nuclear force has no effect. This process is known as the direct break up.

In the intermediate energy range it may be possible to observe the transition between the sequential and direct break up processes. But the observation of the direct break up is only possible if the projectile has a large energy gap between its break up threshold and its next quasi–bound state. Then the break up events corresponding to this energy gap can be identified as direct events. The events

with relative energy corresponding to the next excited state are taken as the sequential events.

^7Li has an α+t threshold of 2.46 MeV with its next excited state, $J^\pi = 7/2^-$ resonance, at 4.63 MeV. Hence an energy gap of $\simeq$ 2.16 MeV and the events corresponding to this energy can be easily measured. Furthermore its cluster structure simplifies the calculations considerably and makes ^7Li a particularly interesting nucleus for Coulomb break up studies.

In this chapter previous works done on this subject are discussed and the calculations of break up cross section based on the method used in this thesis are presented. Section 6.2 is a brief account of the experimental and theoretical work up-to-date. The model calculations are discussed in Section 6.3 and the results are compared with data in Section 6.4. The final section is a summary of the conclusions.

6.2 Break up Studies

A series of interesting experiments on break up of ^7Li was performed by the Edinburgh group (Shotter *et al*, 1981-1987) with parallel theoretical work to try to understand the experimental results. In these experiments a particular detector geometry is used which enables the measurement of the break up cross sections at very small angles. The α particle and the triton are recorded in separate detectors and the coincidence events with an $\alpha - t$ relative energy less than 2.1 MeV are recorded as direct break up events. The events with relative energy of 2.16 MeV are recorded as sequential events.

In one of the earlier experiments (Shotter *et al*, 1981) the break up of ^7Li on ^{12}C and ^{208}Pb at a projectile energy of 70 MeV was studied. The spectra are

dominated by peaks corresponding to the 4.63 MeV state. That is, the summed energy (E_α+E_t) spectrum contains a large peak corresponding to 4.63 MeV. The t (or α) projected spectrum is dominated by two peaks which correspond to the two allowed t (or α) energies from the break up of $^7Li^*$ (4.63 MeV). The events between these peaks can not be related to a discrete state of ^7Li and hence they are assumed to be direct break up events. However almost no events are observed in this region for the break up of ^7Li on ^{12}C at 15° and on ^{208}Pb at 32°. But the triton energy spectrum for ^{208}Pb at 18° contains many events between these peaks, corresponding to the 2.1 MeV relative energy region. They conclude that the break up on ^{12}C is predominantly sequential whereas that on ^{208}Pb has two components; direct and sequential.

Thompson and Nagarajan (1983) have used the DWBA method to study the effect of the Coulomb interaction in the above experiment. But the calculated cross sections are too large , by a factor of 20, when the nuclear forces alone are used. The inclusion of the Coulomb interaction results in an overestimation of the cross section by a factor of 40. This is taken as evidence that a more realistic three body calculations involving the break up states should be performed. The high energy adiabatic approximation of Johnson and Soper (1970) can be used for the treatment of the nuclear force but it is not valid for long range Coulomb interaction. They consider such treatment and improve the results of the nuclear break up obtained by the DWBA method. Finally by including the non-adiabatic approximations they obtain very good results for the above data but only if the Coulomb force is ignored altogether.

Davinson *et al* (1984) have tested the adiabatic approximation by applying it to the inelastic scattering of ^7Li. The first excited state of ^7Li is not a break

up state but the excitation process is the same. So it should provide a good check for the adiabatic method and the effect of the Coulomb interaction on the break up. The excitation of ^{7}Li by ^{208}Pb at 68 MeV has been studied. First they perform a coupled channel calculation involving the ground state and the first excited states only. The result is greatly improved when the Coulomb force is included in the calculation and the data is almost reproduced beyond 30° scattering angle. However at forward angles large oscillations , corresponding to the nuclear–Coulomb interference, are produced, which are not observed. Then the high energy adiabatic approximation is used to perform a coupled channel calculation involving the break up states of ^{7}Li as well. Again the inclusion of the Coulomb force improves the results beyond 30° as well as between 15°–20° but it does not affect the values between 22°–28°. They conclude that in spite of the results of the above calculations (Thompson and Nagarajan, 1983) the Coulomb force plays an important role in the break up of ^{7}Li, but these calculations predict either a large Coulomb cross section or an incorrect nuclear–Coulomb phase difference. This again is taken as evidence for the need of a better treatment of a system of charged particles in the Coulomb field.

The CDCC calculations of Kamimura *et al* (1984) mentioned in chapter 3 are appropriate for a three body problem involving the nuclear force only. In fact they have applied it to the elastic scattering of ^{7}Li from ^{48}Ca at 89 MeV (Kamimura *et al*, 1984) to demonstrate the effect of various continuum states on the elastic cross section. The method with a preliminary inclusion of the Coulomb force is also applied to the break up of ^{7}Li from ^{208}Pb and ^{120}Sn at 70 MeV (Sakuragi, 1986). But it predicts large magnitude for these cross sections. These calculations will be discussed in more details Section 6.4.

The direct break up effects were further studied (Shotter *et al*, 1984) in an experiment with ^{7}Li on ^{120}Sn at 70 MeV and a range of scattering angles. Here again the α energy spectra for backward angles are dominated by the sequential peaks but the events between these peaks become more intense towards forward angles. They suggest that the break up of ^{7}Li at forward angles may be dominated by Coulomb interaction. This idea is also supported by the fact that the distance of closest approach ($\simeq$17 fm) is larger than the radius of appreciable nuclear interaction ($\simeq$13 fm) although this difference is not large enough to rule out the nuclear effects entirely. To test this idea they have calculated the break up cross section on the basis of Coulomb interaction only.

They use a first order perturbation theory to calculate the contribution of E1 transitions to the continuum states. These calculations require the value of the reduced transition probability which is a function of relative energy and can be determined from the photodisintegration cross section. But the data for these cross sections are not available for relative energies below $\simeq$10 MeV. However, the inverse fusion cross section is related to the photodisintegration cross section by a reciprocity relation (Blatt and Weisskopf, 1952) and is used to calculate the reduced transition probabilities. The resulting calculated cross sections are in close agreement with the break up data at the most forward angle. However there are large uncertainties in the calculated values and this agreement does not rule out higher order Coulomb effects.

Following these interesting results another set of experiments was carried out in order to get better insight into the Coulomb effects on the direct break up of ^{7}Li. The break up cross sections were measured for ^{7}Li on ^{208}Pb, ^{120}Sn

and ^{96}Zr at 70 MeV and a range of scattering angles. The higher charge of the target may allow a pure Coulomb process at high energies since the Coulomb barrier is higher. On the other hand a heavier target also has a larger radius of nuclear interaction and hence the result may not be a pure Coulomb interaction. In these experiments both the direct and sequential cross sections are measured. The results for direct break up seems to support the idea of Coulomb break up at forward angles except for the surprisingly large cross section for ^{208}Pb.

These measurements are repeated at the most forward angles (Shotter *et al* , 1987) and at 50, 60 and 70 MeV projectile energy. But again the direct break up cross section for ^{208}Pb seems to be too large at all energies. The calculations performed on the basis of the perturbation theory mentioned above (Shotter *et al*, 1984) also give reasonable results as compared to the data but they greatly underpredict the cross section for ^{208}Pb.

The results of all these experiments and calculations point to the need for a proper treatment of Coulomb break up effects in order to be able to explain the data or indeed to establish the extent to which the direct break up at forward angles can be attributed to the Coulomb interaction. The method used in this thesis was basically devised to deal with this situation and has already predicted the virtual Coulomb break up effects successfully.

6.3 Model Calculations

The energy and the wavefunctions of the break up states of ^{7}Li can be easily calculated by the method described in Section 3.4. Then a full coupled channel calculation, involving the Coulomb force only, would give good estimates of the Coulomb break up cross section.

Using equation 3.1 (Wildermuth condition) the angular momenta of the higher (continuum) states are determined. The allowed transitions between these states and the bound states are determined by the electromagnetic transition rules. The lowest order transitions are shown in table (6.1)

2N+L	L	J	π	$\lvert\Delta L\rvert$	$\lvert\Delta J\rvert$	Transition
4	0	1/2	+	1	1	E1
	2	3/2	+	1	0	E1
	2	5/2	+	1	1	E1
	4	7/2	+	3	2	E3
	4	9/2	+	3	3	E3
5	1	1/2	−	0	1	E2
	1	3/2	−	0	0	E2
	3	5/2	−	2	1	E2
	3	7/2	−	2	2	E2
	5	9/2	−	4	3	E4
	5	11/2	−	4	4	E4
6	0	1/2	+	1	1	E1
	2	3/2	+	1	0	E1
	2	5/2	+	1	1	E1
	4	7/2	+	3	2	E3
	4	9/2	+	3	3	E3
	6	11/2	+	5	4	E5
	6	13/2	+	5	5	E5

Table 6.1

Allowed transitions between the ground state of ^7Li and the continuum states.

The important contributions to the break up cross section come from E1 and E2 components only and the higher order transitions would have negligible effects. The energies and wavefunctions for the states given in Table 6.1 which are involved in such transitions are calculated in a box radius of 20 fm and for a cutoff energy of 20 MeV. The result is 47 continuum states as follows:

J^π	$1/2^+$	$3/2^+$	$5/2^+$	$1/2^-$	$3/2^-$	$5/2^-$	$7/2^-$
no of states	7	7	7	6	6	7	7

There are E1 and E2 transitions also possible between some of these states and the first excited state $J^\pi = 1/2^-$ and the coupled channel calculations include these transitions as well. The transitions between the continuum states themselves were included but, as expected, they did not affect the cross sections. This is due to the fact that the transitions between the continuum states merely redistribute the cross section within these states but do not affect the total cross section. This result also confirms the idea that, since the total effect is considered, a specialized normalisation of the individual states is not required.

It is also important to note that the 7 continuum states with $J^\pi = 7/2^-$ are in effect the same as the $7/2^-$ resonance state at 4.63 MeV and similarly the $5/2^-$ states are the same as the $5/2^-$ resonance. This was discussed with respect to the normalisation of the continuum states in Section 3.5. Hence if either the 7 continuum states or the resonance state are included in the calculations the result should be the same. This is indeed confirmed by the calculation as the resulting

cross sections were very close. It is also clearly demonstrated by the wavefunction of these states compared to that of the resonance state, plotted in figure 6.1. Hence in order to save computing time the resonance states were included instead of the continuum states and also transitions between the continuum states were neglected. So in all the subsequent calculations 37 states are used altogether. Then the direct break up cross section is obtained by adding the cross sections for the transitions to the continuum states with energies below the resonance state at 4.63 MeV. The sequential break up cross section is the cross section to this state itself.

The computer code COULVAR is designed to cope with a maximum of 30 states with the option to increase this number via 3 parameters only (Section 2.6). This option was used to increase the maximum number to 50 states but the results were very disappointing. That is, a very large cross section was obtained that could not be explained on any basis. Fortunately this problem was related to the code but it halted the calculations for a long time as the source of the error was not known. But after detailed examination the error was found to be due to this parameterisation option, and after it was corrected a reasonable cross section was calculated.

Having got over this difficulty the break up calculations for all the available data mentioned above were performed and very interesting results were obtained.

6.4 Comparison with Data

The calculated cross sections for break up from various targets at 70 MeV are plotted, together with the experimental results, in Figures 6.2–6.4. For the

lightest target, ^{96}Zr, the calculated cross section for direct break up is very close to the measured value at the most forward angle. Of course a good agreement, if any, is only expected for the most forward angles where the evidence of strong Coulomb break up has been observed. The cross section for sequential break up is slightly overpredicted but the shape is well reproduced up to 15°.

In the case of ^{120}Sn the cross section for direct break up is much smaller than the experimental value for 11° but becomes very close to data at 15°. This result is quite different from the calculations of Shotter *et al* (1984) using the inverse scattering data. However the cross section for the sequential break up seems to be reasonable up to 18°, becoming very close at this point. The odd feature of these results is the value at 11° where a value slightly smaller than data would be expected rather than slightly larger.

Perhaps the most interesting result are the values for ^{208}Pb. In spite of its large Z value there seem to be no agreement between the calculated and measured values. In both cases, direct and sequential break up, the calculated cross sections are too small at the most forward angle and too large at larger angles. The value for direct break up has the worst disagreement. This clearly rules out a pure Coulomb break up for this case and it will be further discussed in the next section. It is interesting to discuss the CDCC calculations for these cases, at this stage. It was briefly mentioned in Section 6.2 that they have included a Coulomb interaction but overestimated the cross sections. In fact they have only included the resonance states in their coupled channel calculations. The Coulomb interactions are included by folding the nuclear– target potential with the transition densities between the states of ^{7}Li. The inclusion of the

Coulomb force improves the results in that the shape of the cross sections is well produced but the magnitudes are too large by a factor of 3 for ^{120}Sn and by a factor of 4 for ^{208}Pb. They predict that the inclusion of the non resonance states would produce the correct magnitude. As a whole this model does not seem to be useful , as it stands, for interactions involving strong Coulomb force.

The calculated and experimental results for the direct break up from these targets at the most forward angles and at different energies are plotted in Figure 6.5. It should be noted that the scattering angles are slightly different for each target. This is due to the experimental arrangements and the cross sections are measured at the smallest possible scattering angle in each case. The laboratory angles are: 13°, 12°,11° for ^{208}Pb, 13.5°,12.5°, 11.5° for ^{120}Sn and 13°,12°and 10.5° at 50, 60 and 70 MeV respectively. Here again the results for ^{96}Zr and ^{120}Sn are within good agreement in all cases with a slight deviation for ^{120}Sn at 70 MeV. In the case of ^{208}Pb the calculated value is reasonable at 50 MeV but is greatly underpredicted otherwise, more so towards the higher energies.

6.5 Summary and Discussions

These calculations are the best available method to determine the Coulomb break up cross sections. Hence the results can be used to identify the region of pure Coulomb interaction. The comparison with break up data at different energies appears to show a marked difference between the behaviour of the cross sections for ^{208}Pb and other targets. This might imply that the mechanism involved in this reaction is different from assumed interactions, but there is no reason that this target should be so different from the others.

In fact a more careful study of the results show that the deviation of the calculated cross section from the data, which is so strong in the case of ^{208}Pb, also exists in the case of ^{120}Sn. But since the deviation is smaller it is taken as reasonable agreement for ^{120}Sn. The important point is that although the calculated value for ^{120}Sn is reasonable it is smaller than the data, whereas at lower energies (Figure 6.5) where the nuclear force is weaker, the calculated value is slightly larger than data. It is this pattern which is also observed for ^{208}Pb only stronger since a heavier target has a larger radius of nuclear interaction. These results clearly demonstrate that even at the most forward angles and at such high energies the interaction is not necessarily a pure Coulomb force and the nuclear interaction may be significant, depending on the target. The calculated values show the onset of Coulomb-nuclear interference clearly. Figure 6.5 shows that there is no nuclear interference in the case of ^{96}Zr nor in the case of ^{120}Sn at lower energies. But the interference is coming into effect for ^{120}Sn at 70 MeV and also for ^{208}Pb with the nuclear force getting stronger towards higher energies.

One of the reasons that the effect of nuclear interactions was ruled out was the fact that the distance of closest approach for the most forward angle at 70 MeV is $\simeq 29fm$ which is much larger than the radius of nuclear interaction $\simeq 13fm$. But the distance of closest approach is calculated for a Coulomb orbit corresponding to the given scattering angle. If the nuclear force is already active the coulomb orbit which would correspond to a larger scattering angle would be deflected and therefore a small scattering angle is measured.

Another point which might raise the question of a difference between the ^{208}Pb and the ^{120}Sn behaviour is that the measured values for ^{208}Pb at 70 MeV

(Figure 6.4) are oscillatory compared to the values for ^{120}Sn (Figure 6.3) which are monotonically decreasing. But this can also be explained on the basis of nuclear-Coulomb interference. The inelastic scattering data show (Davinson *et al*,1984) that the oscillations which are characteristic of this interference become more enhanced towards forward angles. The grazing angle for ^{208}Pb under these conditions is about 30° and for ^{120}Sn is about 22°. The angle for which the break up data is taken is around 11°. This is clearly much more forward of the ^{208}Pb grazing angle than it is for ^{120}Sn. Hence the oscillations are observed for ^{208}Pb but not for ^{120}Sn. If the measurement of the cross sections for ^{120}Sn around 5° were possible then such oscillations may well be observed.

It is also interesting to compare these oscillations with those observed for heavy ion scattering. These oscillations are known to follow a Coulomb-nuclear phase rule for angles forward of the grazing angle (Brink, 1975). The rule states that the oscillations for excitation by different multipoles should be in phase with each other and out of phase with the elastic Coulomb scattering. A good example of such oscillations is the cross section for $^{14}C+^{88}Sr$ at 51 MeV (Hansen *et al*, 1957) which clearly demonstrate the phase rule. The data for elastic scattering of ^{7}Li on ^{208}Pb at 68 MeV (Davinson *et al*, 1984) and the break up data for the same case (Shotter *et al*,1981) are plotted in Figure 6.6 and have interesting features with respect to the phase rule. The elastic scattering data has a maximum at $\simeq 20°$ and the break up data has a minimum at this point. This is a clear signature of the Coulomb–nuclear interference. Although this case is different from heavy–ion scattering, in terms of the properties corresponding to a Coulomb excitation process they are very similar. For example the radius

of strong interaction is $\simeq$ 11 fm for $^{7}Li +^{208} Pb$ and $\simeq$ 10 fm for $^{14}C +^{88} Sr$. The corresponding Coulomb barrier for both cases is around 32 MeV.

In summary there is no evidence that these large cross sections are due to Coulomb excitation only and some of the measured values clearly involve nuclear excitation as well. Therefore the pure Coulomb interaction is responsible for direct break up at forward angles only for lighter nuclei or lower energies. In the case of heavier targets or high energies such as ^{208}Pb at 70 MeV the Coulomb force, though strong, is not dominant and the observed scattering angle should not be taken as the angle of a classical Rutherford orbit. A full coupled channel calculation involving both the nuclear and Coulomb force should yield a value close to the measured cross section.

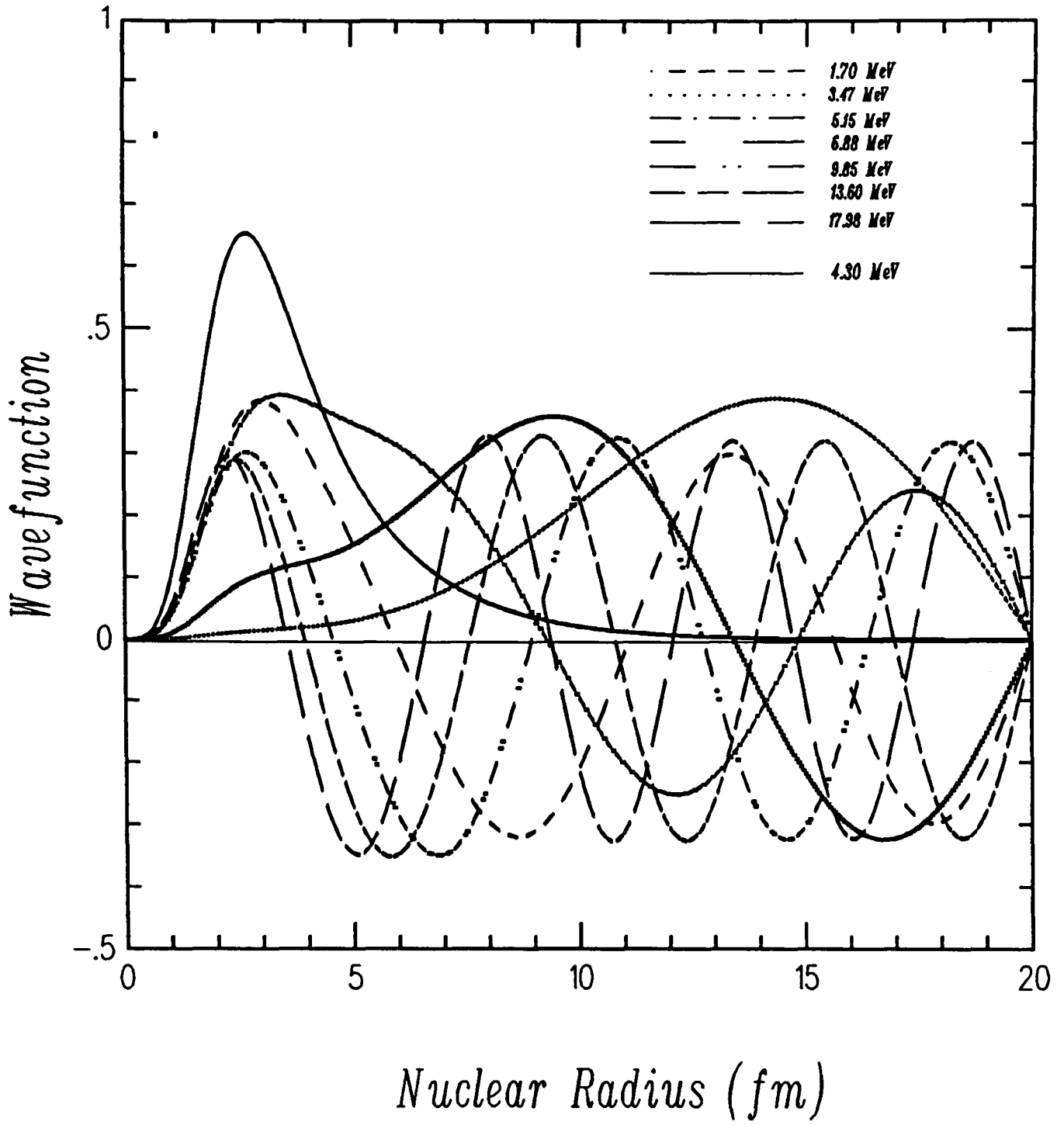

Figure 6.1

The Wavefunctions of the $7/2^-$ continuum states up to 20 MeV and the $7/2^-$ resonance state (4.30 MeV). The bound states wavefunction is negligible for $r > 7fm$ (Figure 3.2).

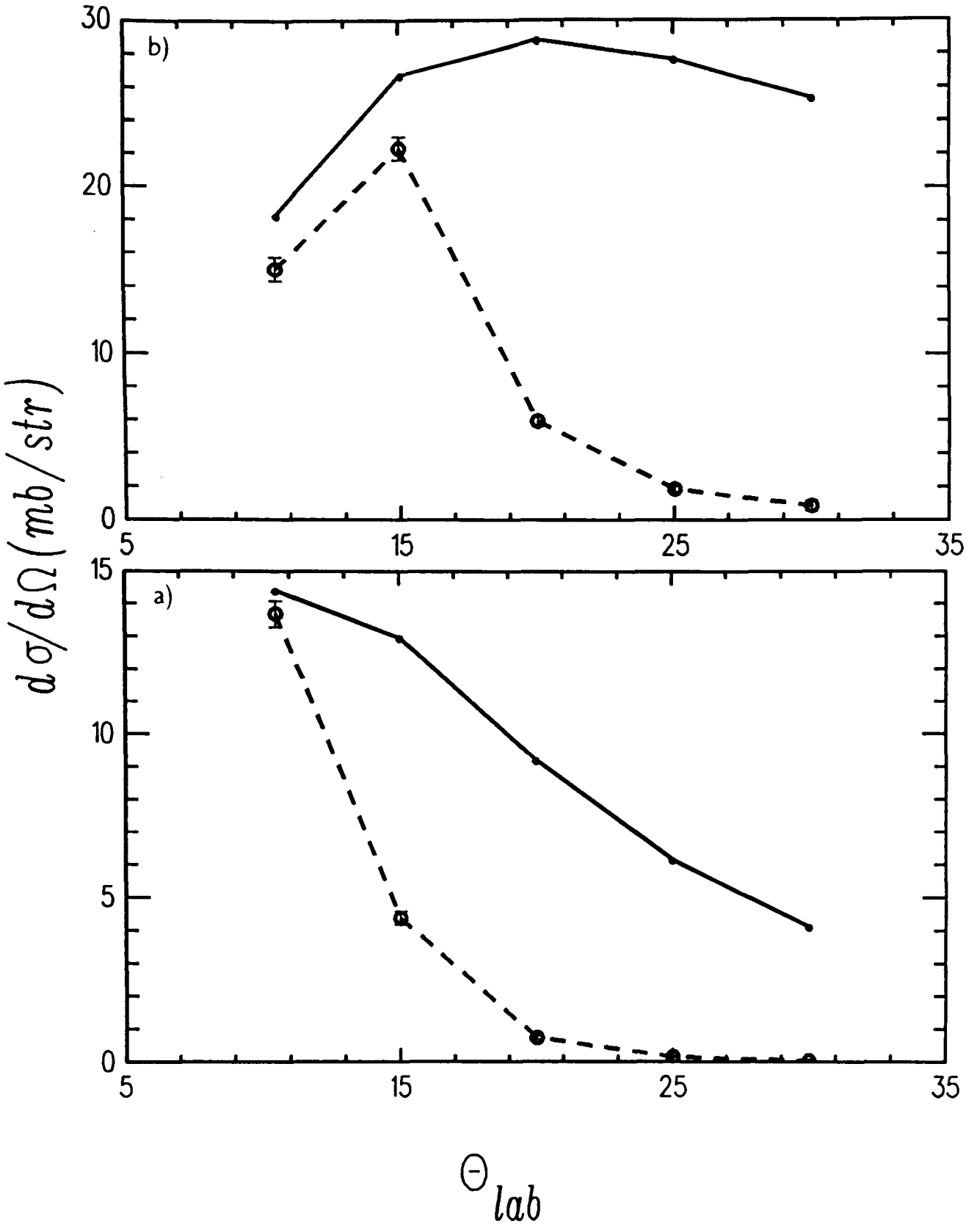

Figure 6.2

The direct (**a**) and sequential (**b**) break up cross sections for $^{7}Li +^{96} Zr$ at 70 MeV. Data from Shotter *et al* (1986).

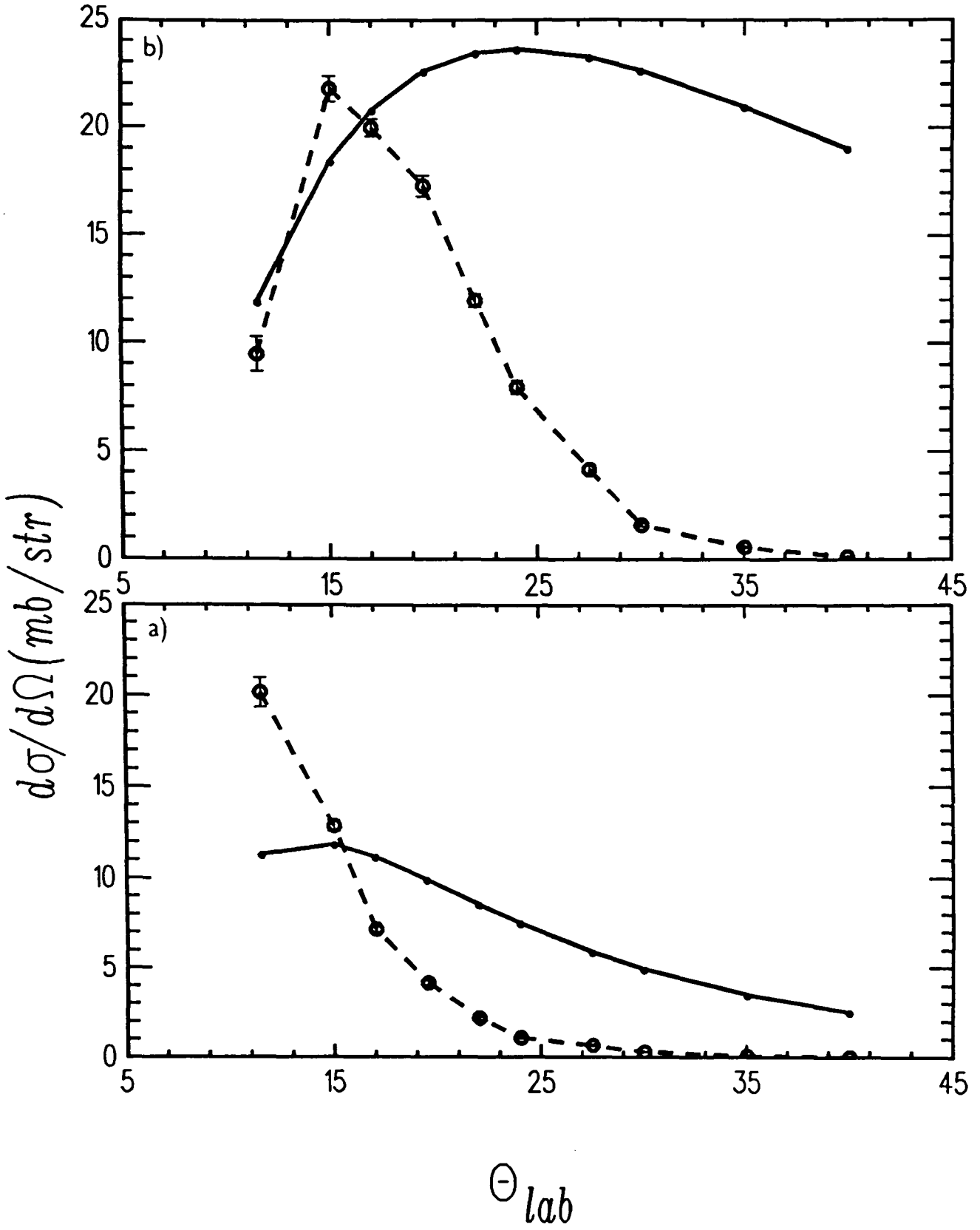

Figure 6.3

The direct (**a**) and the sequential (**b**) break up cross sections for $^{7}Li + ^{120}Sn$ at 70 MeV. Data from Shotter *et al* (1986).

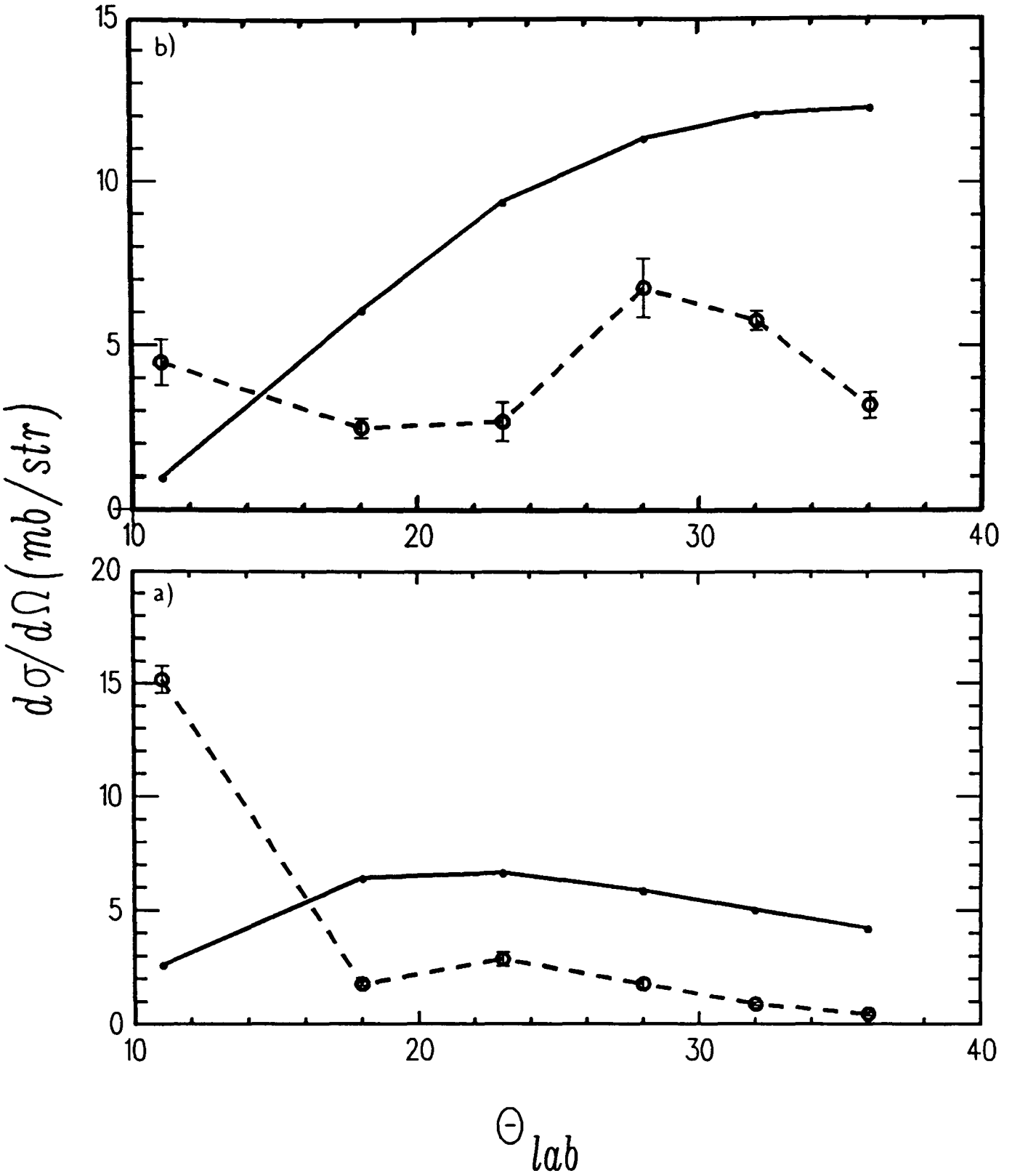

Figure 6.4

The direct (**a**) and the sequential (**b**) break up cross sections for $^{7}Li + ^{208}Pb$ at 70 MeV. Data from Shotter *et al* (1986).

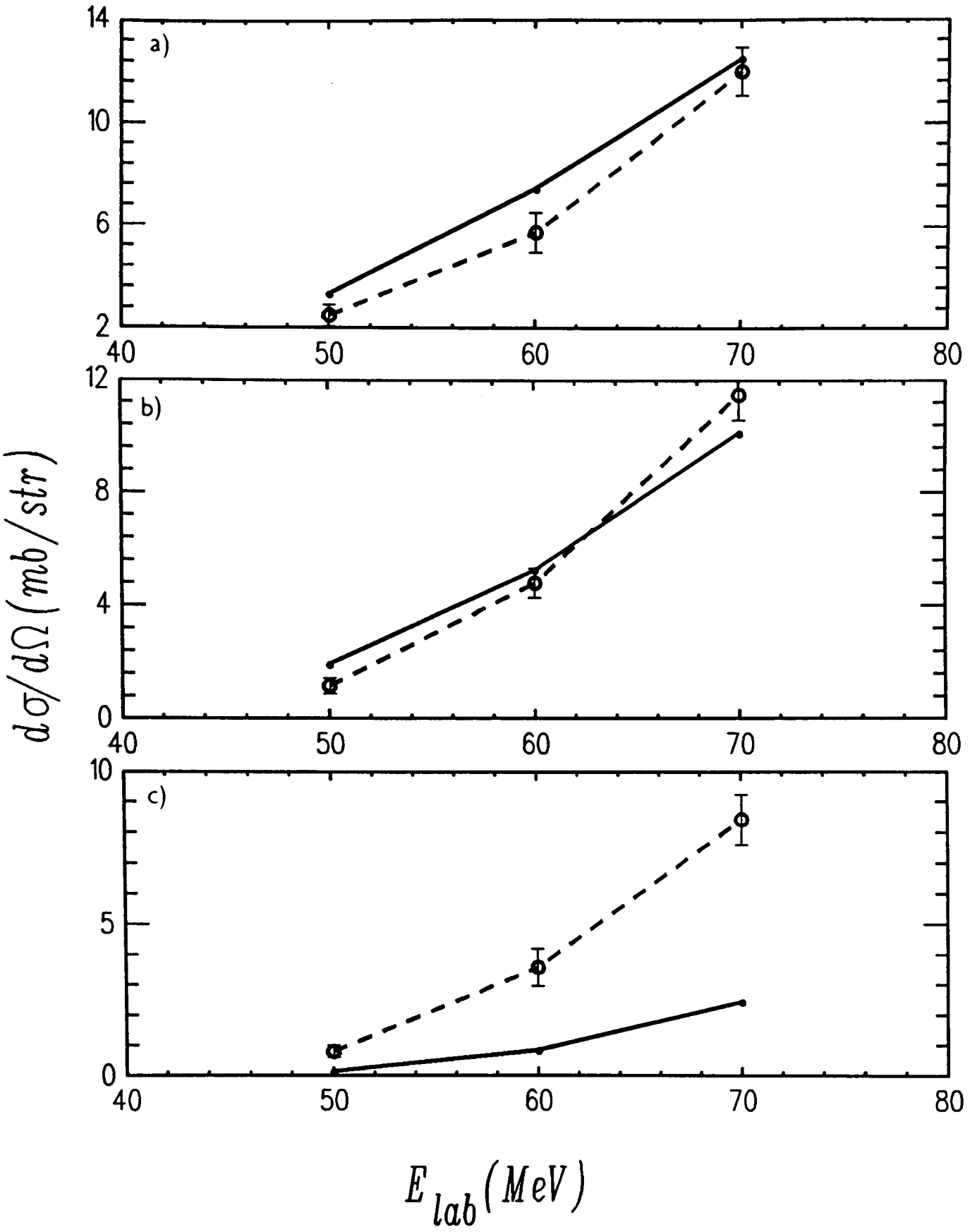

Figure 6.5

The direct break up cross sections for $^7Li +^{96} Zr$ (**a**), $^7Li +^{120} Sn$ (**b**) and $^7Li +^{208} Pb$ (**c**) at most forward angles (Section 6.4). Data from Shotter *et al* (1986).

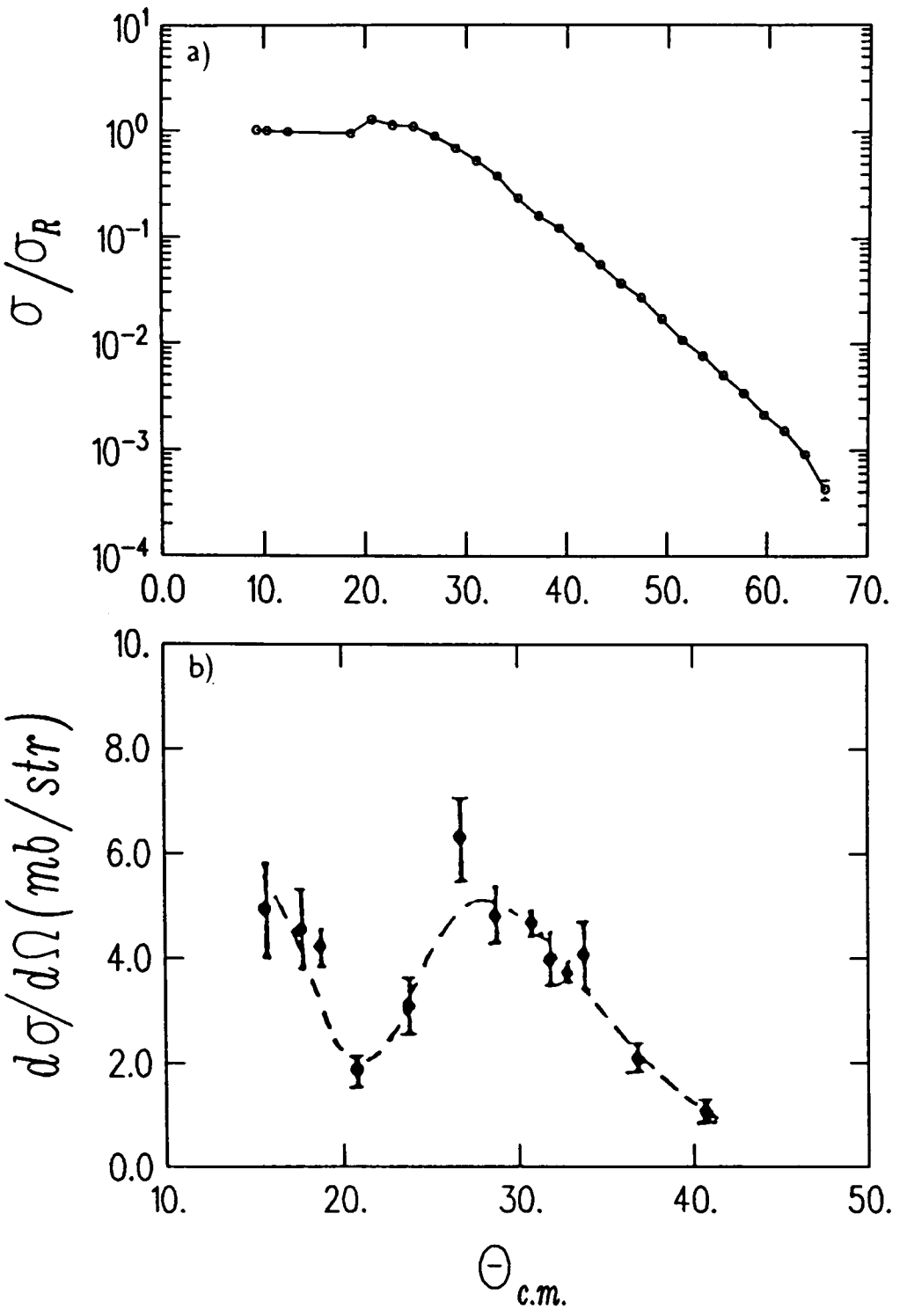

Figure 6.6

The elastic (**a**) and break up (**b**) cross sections for $^7Li + ^{208}Pb$ at high energies. Data is (**a**) from Davinson *et al* (1984) and (**b**) from Shotter *et al* (1981).

Chapter 7

SUMMARY AND DISCUSSION

The aim of the work, reported in this thesis, to develop a realistic model for a three body system interacting in a Coulomb field, is successfully achieved. In this chapter the overall results of this work are summarised. In the following section a summary of the method and the result of its application to the inelastic scattering of ^7Li is presented. In Section 7.2 the approximate treatment of the Coulomb–nuclear interference at low energies and its achievements are listed. The break up results are discussed in Section 7.3 and finally the possible improvements of the method together with its future applications are suggested in Section 7.4.

7.1 The Continuum States of the $\alpha + t$ System

The idea of confining the two particles to a spherical box has produced a very simple and reliable method to treat the continuum states of such system. The reproduction of various experimental data presented in Section 4.3 is strong evidence for the reliability and accuracy of the method. Bearing in mind that

due to different treatments of continuum states the values extracted by these experimental data do not agree, this is a great achievement.

On this basis one can suggest with some degree of confidence that this is the best available model independent method for calculations involving three body problems (two of these particles should remain close together). In the case of ^7Li it has successfully cleared up the discrepancy between the $B(E2)$ values and, since it predicts the correct E1 contribution to the excitation states it can be used to extract an accurate $Q_{3/2^-}$ value. This has been the subject of various recent studies. It was suggested (Sundholm *et al*, 1984) that the Hartree–Fock method used (Green, 1971) to extract the static quadrupole moment from the atomic beam spectroscopy is not accurate and the actual value should be -4.06 ± 0.03 e fm^2 rather than the previous value of -3.66 ± 0.08 e fm^2. The revised calculations of the SCM (Buck and Merchant, 1988) also predict a higher $Q_{3/2^-}$ value of -3.83 ± 0.13 compared to the previous calculations (Buck *et al*, 1984). In fact this recent extracted value (Sundholm *et al*, 1984) is even closer to the value extracted by Vermeer *et al* (1984) hence supporting the large E1 contribution measured in the same experiment and also predicted by the calculations in this thesis.

However the application of the proposed three body model is by no means restricted to ^7Li or the SCM. In general it can be applied to all the cluster–like nuclei and any cluster model as long as the cluster separation during the interaction satisfies the basic assumption of the model discussed in Section 3.3. Hence in the case of a well known nuclear model the method can be used to calculate the effect of events which are strongly coupled to the continuum states

and in the case of the accurately measured properties involving the continuum states the method can be used to test the nuclear models.

This method has a number of advantages over the CDCC method of Kamimura *et al* (1984). Its most important advantage is that it treats the Coulomb force realistically and therefore is particularly useful for pure Coulomb break up processes, real or virtual. It can also cope with more states than the CDCC model as it does not impose any restriction on the maximum angular momentum of the continuum states. In fact in the calculation of the elastic and the inelastic cross sections of ^{7}Li they have only included the P-states (L=1) and the F-states (L=3). They assume (Kamimura *et al*, 1984) that the coupling to the S-states (L=0) and the D-states (L=2) are negligible for these calculations. This assumption may be valid for nuclear interaction but not for the Coulomb force. The calculations presented in chapter 4 suggest quite the opposite as the only important contribution to the virtual break up comes from the S-states (L=0) and some of the the D-states (L=2).

Another important point is that they have used different model spaces for these calculations and the break up calculations (Kamimura *et al*, 1986). That is, the width of the momentum bins is different and also variable in the case of break up calculations. Whereas the method presented here uses the same parameters for all the calculations, virtual or real break up.

The only advantage of the CDCC method is that the continuum states are properly normalised with respect to the width of the momentum bins. For example the $7/2^{-}$ states consist of three bins (Kamimura *et al* , 1984) one of which corresponds to the $7/2^{-}$ resonance with correct energy and the other

two are the non resonance states corresponding to the background discussed in Section 3.4. But the normalisation of the states in the proposed method can be easily achieved and will be discussed in Section 7.4. The inadequacy of the CDCC method in dealing with strong Coulomb break up will also be discussed later in the relevant section.

7.2 Nuclear–Coulomb interference

These calculations, have produced good results and demonstrate the validity of the technique (chapter 5). The approximate method used to treat these interferences at low energies proved to be justified and reliable. Although clearly other improvements were needed to obtain the correct interference, such improvements, namely the renormalisation of the nuclear potentials, were already known to be necessary for this region from other independent studies (Mackintosh *et al*, 1982–1986). The reproduction of the inelastic scattering data in the region of a weak nuclear interference (Figures 5.4 and 5.5), which were obtained by refitting the nuclear potentials is strong evidence for the success of the proposed approximation. The shape of the refitted potentials also agrees with the the conclusions of the inverse scattering calculation by Mackintosh *et al.*

As a result of such good agreement with the data, it is clear that this is a new method for determining the nuclear potentials at large radii. The nuclear scattering experiments do not provide any information about the nuclear potential at large distances and the inverse scattering calculations cannot, as yet, be applied to the nuclei with half integer spin ground state. But the Coulomb scattering data can be used to determine the long range behaviour of the nuclear potentials for many nuclei.

It should be strongly emphasised that such refitted potentials only represent the nuclear potential in the surface region. Hence the information obtained by the refitting procedure together with that obtained from the nuclear scattering provide a well determined potential over a long range.

It is also worth mentioning that the nuclear forces do not seem to be strong enough, at these energies, to affect the orbit of the projectile. This is confirmed by the good fits obtained for this region. If the orbit was affected by the nuclear force then the refitting of the nuclear potentials alone would not provide a good fit to data. This point is clearly demonstrated by the break up data which will be discussed in the next section.

7.3 Break up Calculations

Perhaps the most interesting results of the application of the three body method are the calculated break up cross sections. Although the method is very useful for the analysis of the inelastic scattering data, it plays a far more important role in the analysis of the break up of ^{7}Li. Various experiments by Shotter *et al* (1981, 1984) strongly suggested that the break up of ^{7}Li on heavy targets at high energies is dominated by the Coulomb force at the most forward angle. However the experiment with ^{208}Pb, aiming to confirm this dominance in the direct break up processes, shows evidence of the nuclear interference. The puzzling feature was the close agreement of the calculated cross sections for the break up on ^{120}Sn under similar conditions (Shotter *et al*, 1984). The calculations performed by including all the relevant continuum states which contribute to the break up cross section provide a reliable estimate of the

Coulomb break up cross section and solve the problem. The results of these calculations are slightly different from the approximate calculation of Shotter *et al* for ^{120}Sn but are still close to the measured value. However the discrepancy with data increases for ^{208}Pb especially at higher energies. The conclusions based on these results are as follows:

The break up of ^{7}Li on ^{96}Zr at the most forward angles is dominated by the Coulomb force even at high energies (70 MeV).

The break up on ^{120}Sn at the most forward angle is a pure Coulomb process at lower energies but at 70 MeV the nuclear interference is evident. However the nuclear force is still relatively small so the orbit of the particle is not affected and a reasonable agreement with the data is obtained.

The break up on ^{208}Pb has all the features of a strong nuclear interference even at the most forward angles. The surprisingly small measured cross section compared to the large calculated value (at 70 MeV) and also the large oscillation in the cross section at forward angles which is typical of strong nuclear interference are evidence for a considerable effect from the nuclear force. This is also confirmed by the fact that when the approximation used for the nuclear–Coulomb interference at low energies was applied to this case the calculated cross section is not affected. This clearly shows that the nuclear force can not be merely treated as a perturbation to the Coulomb force and the Coulomb orbit is also disturbed.

The distance of closest approach for these conditions is $\simeq$ 29 fm but the evidence suggests that the target comes well within the range of nuclear interaction at $\simeq$ 13 fm. Therefore the observed scattering angle which leads to this

large distance of closest approach should not be taken as the scattering angle of a Coulomb orbit and it is the angle of a distorted orbit.

Obviously for this case a full coupled channel calculation involving both the Coulomb force and the nuclear force is required. It should be noted that the Coulomb force is still strong and should be treated properly. In fact the CDCC method has been used to calculate these cross sections (Sakuragi *et al* , 1986) but it overpredicts the break up cross sections. Although the preliminary inclusion of the Coulomb force greatly improves the results and reproduces the shape of the measured cross section the magnitudes are too large for both cases, ^{120}Sn and ^{208}Pb. In principle the method for continuum states can also be used to cope with such calculations as it will be discussed in the next section.

7.4 Improvements and further applications

7.4.1 Normalisation

It is interesting to include the normalisation of the continuum states with respect to their density in an energy interval in the method used to calculate these states. This is not necessary for the any of the calculations discussed in this work or similar studies. But as a generalisation of the method it would be useful and makes the method also useful for phase shift calculations.

At present the continuum states are obtained by scanning an energy range and looking for energies at which their corresponding wavefunctions will go to zero at the box radius (Section 3.4). This is an arbitrary boundary condition chosen for simplicity. For the normalisation purpose the boundary condition can be chosen such that the wavefunction at the box radius is matched to a

linear combination of Coulomb functions. Then the logarithmic derivative of the wavefunction which is already calculated in the method, is related to the scattering phase shift (Jackson, 1970) and they can be matched to obtain the required boundary condition for the continuum states. Then the energy range is scanned to look for the energies at which their corresponding wavefunction match this boundary condition. The states thus obtained may have the same density as before but a single state at the required energy will be obtained. This procedure can be easily included in the model hence obtaining a normalised wavefunction for any required scattering state.

7.4.2 Even Parity Potentials of SCM

The main advantage of the proposed method for the continuum states is that it correctly predicts the virtual break up effects. This advantage can be used to determine a unique potential for the even parity states of ^7Li in the Simple Cluster Model. The potential parameters used for the calculation of the L=0 continuum states were obtained by fitting the phase shift of these states. But only the depth was varied and the results of the calculations suggest that better fitted potentials, producing slightly larger matrix elements are required to fit the inelastic scattering data. A good fit to the phase shift can also be obtained by varying the shape of the potential as well as the depth ,thus producing the required matrix elements. Therefore if the search for the best fit potential to the scattering phase shift is linked with the calculation of the Coulomb excitation probabilities the potentials of S–states can be better determined.

7.4.3 Inclusion of the Nuclear Interactions

As mentioned before the object of the calculations performed in this thesis was to determine the Coulomb break up effects. Hence the nuclear interactions were only considered as a perturbation to the Coulomb force. However this approximation is only valid for low energies where the Coulomb force is dominant. It would be both interesting and useful to be able to include the nuclear interactions when they are strong as well. The immediate application of such improvement is the calculation of the break up cross section of ^{7}Li on ^{208}Pb discussed above. The continuum states obtained by the proposed method can be easily included in full coupled channel calculations involving both of the interactions. However a Coulomb excitation code is not suitable for such calculations as it is based on the Coulomb orbits. Then a specific code is required to calculate the excitation probability for a process involving both the Coulomb and the nuclear interactions in the framework of the three body model. This is not difficult but restrictions may be needed to be imposed on the number of continuum states as the calculations are more complicated and lengthy.

An easy way of performing such calculations is to use the Taylor expansion of the interaction between the target and the projectile in terms of the cluster–target interactions involved in the excitation process. Then the leading term will contain such interactions evaluated at a radius equal to the separation between the centres of mass of the target and the projectile. The first order term contains the gradients of these interaction evaluated at the same radius etc. These interactions are of course the combination of Coulomb and nuclear

forces, hence both these interactions are included in the three body system. If such a code is developed its application is not restricted to the case of ^{7}Li only and can be generalised so that it is applicable to all the break up calculations involving three body problems and strong Coulomb force.

REFERENCES

AHRENS J., BORCHERT H., CZOCK K. H.,EPPLER H. B., GIMM H., GUNDRUM H., KRÖNING M., RIEHN P., SITA RAM G., ZIEGER A. and ZIEGLER B. 1975, *Nucl. Phys.* **A251** 479.

ALDER K., BOHR A., HUUS T., MOTTELSON B. and WINTHER A. 1956, *Rev. Mod. Phys.* **28** 432. Reprinted in ALDER and WINTHER (1966).

ALDER K. and WINTHER A., (Eds.) 1966, " Coulomb Excitation", Academic Press, New York.

ALDER K. and WINTHER A, (Eds.) 1975, " Electromagnetic Excitation with Heavy Ions", North Holland Publishing Company, Amsterdam–Oxford.

BAMBERGER A., JANSEN G., POVH B., SCHWALM D and SMILANSKY U. 1972, *Nucl. Phys.* **A194** 193.

BARKER F. C. 1982, *Aust. J. Phys.* **35** 291.

BLATT J. M. and WEISSKOPF V. F. 1952, " Theoretical Nuclear Physics", John Wiley and Sons Inc., New York.

BOHR A., and MOTTELSON 1953, *Kgl. Danske Videnskab, Selskab Mat.-Fys. Medd.* **27** no 16.

BOUTEN M. and BOUTEN M. C. 1981, *Prog. part. Nucl. Phys.* **5** 55.

BREIT G., GLUCKSTERN R. L. and RUSSELL J. E. 1956, *Phys. Rev.* **103** 727.

BRINK D. M. 1985, " Semi–classical Methods in Nucleus–Nucleus Scattering ", Cambridge University Press, Cambridge.

BRINK D. M. and SATCHLER G. R. 1968, "Angular Momentum", Clarendon Press, Oxford.

BUCK B. 1984, "Clustering Aspects of Nuclear Structure", Eds. Lilley J. S. and Nagarajan M. A., D. Reidel Publishing Company, Dordrecht–Lancaster.

BUCK B., BALDOCK R. A. and RUBIO J.A. 1985, *J. Phys. G: Nucl. Phys.* **11** L11.

BUCK B. and MERCHANT A. C. 1988, preprint.

DAVINSON T., RAPP V., SHOTTER A. C., BRANFORD D., NAGARAJAN M. A., THOMPSON I. J. and SANDERSON N. E. 1984, *Phys. Lett.* **139B** 150.

De Boer J. 1978, Private Communication.

De Boer J. and Eichler J. 1968, "Advances in Nuclear Physics", Eds. Baranger M. and Vogt E., Plenum Press, New York.

Denisov V. P. and Kulchitskii L. A. 1967, *Sov. J. Nucl. Phys.* **5** 490.

Dirac P. A. M. 1958, "The Principles of Quantum Mechanics", Oxford University Press, Oxford.

Dos Aidos F. D. S. S. 1983, D. Phil. thesis, Oxford.

Eichler J. 1964, *Phys. Rev.* **133** 1162.

Fatemian M., Baldock R. A. and Brink D. M. 1986, *J. Phys. G: Nucl. Phys.* **12** l251.

Fewell M. P., Baxter A. M., Kean D. C., Spear R. H. and Zabel T. H. 1979, *Nucl. Phys.* **A321** 457.

Fiarman S. and Hanna S. S. 1975, *Nucl. Phys.* **A251** 1.

Fiarman S. and Meyerhof W. E. 1973, *Nucl. Phys.* **A206** 1.

Green S. 1971, *Phys. Rev.* **A4** 251.

Hansen O., Videbeck F., Flynn E. R., Peng J. C. and Cizeweski J. A. 1981, *Nucl. Phys.* **A364** 144.

Häusser O., McDonald A. B., Alexander T. K., Ferguson A. J. and Warner R. E. 1973, *Nucl. Phys.* **A212** 613.

Huss T. and Zupancic C. 1953, *Kgl. Danske Videnskab, Selskab, Mat.-Fys. Medd.* **28** no 1. Reprinted in Alder and Winther (1966).

Ioannides A. A. and Mackintosh R. S. 1985, *Phys. Lett.* **161B** 43.

Ioannides A. A. and Mackintosh R. S. 1986, *Phys. Lett.* **169B** 113.

Jackson D. F. 1970, " Nuclear Reactions", Methien & Co. LTD., London.

Johnson R. C. and Soper P. J. R. 1970, *Phys. Rev.* **C1** 976.

Kamimura M., Yahiro M., Iseri Y., Nakano M. and Sakuragi Y. 1984, "Clustering Aspects of Nuclear Structure", Eds. Lilley J. S. and Nagarajan M. A., D. Reidel Publishing Company Dordrecht-Lancaster.

KAMIMURA M., SAKURAGI Y., ISERI Y., YAHIRO M., KAMEYAMA H., KAWAI M and TANIFUJI M. 1986, Proceedings of the International Nuclear Physics Conference, Harrogate, U.K.

LANDOWNE S., DASSO C. H. and POLLAROLO G. 1986, *Phys. Lett.* **178B** 336.

LEVINGER J. S. 1957, *Phys. Rev.* **107** 554.

MACKINTOSH R. S. 1987, Private communication.

MACKINTOSH R. S. and KOBOS A. M. 1982, *Phys. Lett.* **116B** 95.

MCCLELLAND C. L. and GOODMAN C. 1953, *Phys. Rev.* **91** 760. Reprinted in ALDER and WINTHER (1966).

MCDONALD N. 1964, *Phys. Lett.,* **10** 334.

MERZBACHER U. 1961, "Quantum Mechanics", Wiley & Sons Inc., New York.

MESSIAH A., 1956, "Quantum Mechanics", North Holland Publishing Company, Amsterdam.

PEREY C. M. and PEREY F. G. 1976, *Nucl. data* **17** 1.

RUBIO J. A. 1984, D. Phil. thesis, Oxford.

SAKURAGI Y., YAHIRO M. and KAMIMURA M. 1986, *Prog. Theor. Phys. Suppl.* **89** 136.

SHOTTER A. C., BICE A. N., WOUTERS J. M., REA W. D. and CERNY J 1981, *Phys. Rev. Lett.* **46** 12.

SHOTTER A. C., RAPP V., DAVINSON T., BRANFORD D., SANDERSON N. E. and NAGARAJAN M. A. 1984, *Phys. Rev. Lett.* **53,** 1539.

SHOTTER A. C. 1987, Private communication.

SMILANSKY U., POVH B. and TRAXEL K. 1972, *Phys. Lett.,* **38B,** 293.

SUKUMAR C. V. and BRINK D. M. 1983, *Nucl. Phys.* **A404** 121.

SUNDHOLM D., PYYKKÖ P., LAAKSONEN L. and SADLEJ A. J. 1984, *Chem. Phys. Lett.* **112** 1.

THOMPSON I. J. and NAGARAJAN M. A. 1983, *Phys. Lett.* **123B** 379.

TOMBRELLO T. A. and PARKER P. D. 1963, *Phys. Rev.* **131** 2582.

VERMEER W. J., BAXTER A. M., BURNETT S. M., EAST M. T., FEWELL M. P. and SPEAR R. H. 1984, *Aust. J. Phys.* **37** 273.

WELLER A., EGELHOFP., CAPLAR R., KARBAN O., KRÄMER D., MÖBIUS K–H., MOROZ Z., RUSEK K., STEFFENS E., TUNGATE G., BLATT K., KOENING I and FICK D. 1985, *Phys. Rev. Lett.* **55** 480.

WILDERMUTH K. and KANELLOPOULOS TH. 1958/59, *Nucl. Phys.* **9** 449.

WINTHER A. 1966, *Proc. Int. Conf. On Nuclear Physics with Tandems,* Heidelberg.

WINTHER A. and DE BOER J. 1966, California Institute of Technology, Technical Report, November 18. Reprinted in ALDER and WINTHER (1966).

YAHIRO M., NAKANO M., ISERI Y. and KAMIMURA M. 1982, *Prog. Theor. Phys.* **67** 1467.